University of Nairobi

School of Engineering

Identification of Tree Species Using Airborne Hyperspectral Data

A Case study of Ngangao Forest in Taita Hills, Kenya

By

Samuel Mwenje Nthuni

F80/85221/2012

B.Sc. Surveying (University of Nairobi); M.Sc. Geomatics (Karlsruhe University of Applied Sciences)

A thesis submitted in fulfilment for the Degree of Doctor of Philosophy in Geospatial Engineering in the Department of Geospatial and Space Technology of the University of Nairobi

November 2018

Declaration

I, Samuel Mwenje Nthuni, hereby declare that this thesis is my original work. To the best of my knowledge, the work presented here has not been presented for a degree in any other Institution of Higher Learning.

…… ……

Name of student Date

This thesis has been submitted for examination with our approval as university supervisors.

…… ……

Dr.-Ing Faith Karanja Date

…… ……

Prof. Petri Pellikka Date

…… ……

Dr. Mika Siljander Date

Dedication

This research work is dedicated to my wife Lisper and my children Sheila and David

Acknowledgements

I would like to express my appreciation to the Ministry of Foreign Affairs of Finland and International Centre of Insect Physiology and Ecology (ICIPE) for giving me an opportunity to pursue my studies by supporting this research through the CHIESA project coordinated by Dr. Tino Johansson.

I owe special thanks to my supervisors Dr.-Ing Faith Karanja (University of Nairobi), Prof. Petri Pellikka and Dr. Mika Siljander (both from University of Helsinki), who offered me timely guidance and direction throughout the research period. I acknowledge ICIPE, University of Helsinki and University of Nairobi for offering me working space, hardware and software to conduct this research.

I am grateful to Dr. Janne Heiskanen for his professional advice on hyperspectral data processing and analysis during my time at the University of Helsinki. I remain indebted to Dr. Eduardo Maeda, Pekka Hurskainen, Dr. Binyam Hailu, Dr. Mark Boitt, Rami Piirroinen and Arto Viinikka for your support in one way or another during data collection in Taita Hills and data processing in Helsinki.

My appreciation also goes to Kenya Forest Service for allowing me to conduct research in its gazetted Ngangao Forest. Special thanks to Jonam Mwandoe of KFS for his assistance in identification of tree species in Ngangao Forest during my data collection expedition.

Finally, I express my sincere appreciation to my family and friends for their support and encouragement throughout the research period.

Abstract

The impacts of climate change in the African continent have far reaching effects because it is a region of high vulnerability to climate shocks; it threatens food security, livelihoods and biodiversity. African forest ecosystems, which are interlinked to food production systems, are among the most impacted by world climate change. More so, the indigenous tree species are at a high risk of extinction hence the need to quantify them for conservation purposes. Modern methods such as remote sensing and specifically hyperspectral remote sensing offer more accurate methods with expansive scope for conservation, compared to the tedious and time-consuming methods that were previously used. Generally, this study aimed at mapping the indigenous and exotic tree species appearing on the top canopy in Ngangao forest using airborne hyperspectral data. Specifically, it aimed at determining the appropriate wavelengths for mapping of selected tree species; mapping selected tree species using different classification algorithms and the selected appropriate spectral bands; and testing the potential application of simulated multispectral data to discriminate tree species in Ngangao Forest. The Ngangao Forest is located in the Taita Hills in Kenya, approximately 100 km east of Kilimanjaro. The hyperspectral image was acquired using AISA Eagle VNIR sensor and used to map the tree species in Ngangao Forest using different algorithms. Simulated multispectral images with different spatial resolutions were used to map the same tree species and their accuracies compared with those of the hyperspectral images. Classification accuracies of between 49% and 80% were achieved using different machine learning algorithms. Spectral Angle Mapper proved to be the most inferior with an overall accuracy of 49.24% while Random Forest was the most superior with an overall accuracy of 80.00%. Among the species, *Pinus patula* and *Albizia gummifera* were the most accurately mapped while *Macaranga capensis and Phoenix reclinata* were the least accurately mapped. The Random Forest ensemble eliminated redundant bands to achieve an optimal 53-band image for classification. These bands were centred around the blue, green, red-edge and infra-red regions of the electromagnetic spectrum. Simulating multispectral images to Worldview 2 and Sentinel 2, reduced the disk size and processing load on the computer. However, the species identification accuracy reduced while the training and testing sites were considerably fewer as the spatial and spectral resolution reduced. Ultimately, an increment in spectral and spatial resolution increases the species classification accuracy of the tree species in Ngangao Forest. An algorithm with the ability to use fewer training sites and an image resolution that enables one to collect more accurate

end members would achieve higher species classification accuracies using multispectral images. In the absence of this, hyperspectral images provide an alternative to this lacuna.

Table of Contents

List of Tables

List of Figures

List of Acronyms and Abbreviations

AISA:	Airborne Imaging Spectrometer for Applications
ANN:	Artificial Neural Network
ASD:	Analytical Spectral Devices
AVHRR:	Advanced Very High Resolution Radiometer
AVIRIS:	Airborne Visible Infrared Imaging Spectrometer
CHIESA:	Climate Change Impacts on Ecosystem Services and Food Security in Eastern Africa
DEM:	Digital Elevation Model
EABH:	Eastern Afromontane Biodiversity Hotspot
EM:	Electromagnetic Spectrum
GLCC:	Global Land Cover Characterization
GLT:	Geographic Lookup Table
HIS:	hue–saturation–value
HMM:	Hidden Markov Models
ICA:	Independent Component Analysis
LiDAR:	Light Detection and Ranging
MLC:	Maximum Likelihood Classification
MNF:	Minimum Noise Fraction
MODIS:	Moderate Resolution Imaging Spectroradiometer
MSE:	Mean Square Error
NDVI:	Normalized Difference Vegetation Index
NIR:	Near Infra-Red
OA:	Overall Accuracy
OOB:	‘out-of-bag’
PA:	Producer’s Accuracy
PCA:	Principal Component Analysis
PPI:	Pixel Purity Index
RF:	Random Forest
SAM:	Spectral Angle Mapper
SDA:	Stepwise Discriminant Analysis
SVM:	Support Vector Machines

SWIR: Short-wave Infra-Red

UA: User’s Accuracy

VI: Vegetation Index

VNIR: Visible and Near-Infrared

CHAPTER ONE
INTRODUCTION

1.1 Background

The impacts of climate change have been widely felt. The Human Development Report 2007/2008 (UNDP, 2007) identifies Africa as a region of high vulnerability to climatic shocks, where climate change threatens food security, livelihoods and economic prosperity. It has led to increased temperatures and reduction in annual rainfall which have had far reaching effects to biodiversity. Forest ecosystems are among the ecosystems which are and will continue to be severely impacted by the effects of climate change (Robledo et al., 2005).

Forest ecosystems and food production are interlinked at several levels such as; some forest plants produce fruits which can be consumed by human beings, forests regulate the water cycle hence maintaining water-flow into agricultural areas, and also conserve the soil.

This research has been conducted under the Climate Change Impacts on Ecosystem Services and Food Security in Eastern Africa (CHIESA) project. The project was funded by the Ministry of Foreign Affairs of Finland and ICIPE - International Centre of Insect Physiology and Ecology. The objective of the CHIESA project was to fill critical gaps in knowledge related to climate and land change impacts on ecosystem services in the Eastern Afromontane Biodiversity Hotspot (EABH) and develop adaptation strategies towards it through building the capacity of local research and administrative organisations through research, training and dissemination. The project aimed at building the capacity of research communities, extension officers and decision-makers in environmental research in agriculture, hydrology, ecology and geoinformatics; in order to strengthen climate and land use change monitoring and prediction systems and adaptation strategies. CHIESA tackled the project objectives through 8 work packages (WP) that were all interlinked, but which also had their own activities, results and application plans. The WPs were: 1) Coordination and management, 2) Land use and bio-geophysical information, 3) Valuation of ecosystem services, 4) Assessment of impacts on biodiversity and habitats, 5) Assessment of ecosystem pest management and pollination, 6) Assessment of impacts on water provision, 7) Elaboration of adaptation strategies, and 8) Dissemination of the main results and their application.

This research was c under WP2, whose main objective was to use satellite imagery and airborne remote sensing data for land cover mapping and change detection.
The Target areas of the CHIESA project were three mountain areas in EABH in Kenya, Ethiopia and Tanzania. These areas were Taita Hills in South-east Kenya, Pangani river basin in North-East Tanzania and Jimma in South-West Ethiopia. This research focused on one forest patch within Taita Hills i.e. Ngangao with an aim of using airborne hyperspectral imagery to map the distribution of selected tree species.

Mapping of tree species is important for a number of reasons. Some trees species have medicinal value, others are favoured nesting places for particular species of birds, and others are tourist attraction. Taita hills are endowed with rich biodiversity which include a variety of tree and bird species, some of which are endemic in this area. For these reasons, it was necessary to map the extent of these tree species in order to be able to manage them accordingly. Remote sensing techniques for classifying tree species have proven to be valuable in comparison to the tradition methods of mapping tree species (Voss and Sugumaran, 2008).

Forests play a vital role in the regulation of climate and are essential to various cultural, economic and ecosystem services (Thenkabail et al., 2000). It is therefore necessary to sustainably manage and conserve them. Forests in Taita Hills are a key source of herbal medicine, water, sacred places and tourist attraction. Additionally, they are known for their rich biodiversity and are home to three endemic birds and numerous plant species. The Taita Hills form part of the Africa's Eastern Arc Mountains, ranking among the top ten biodiversity hotspots in the world due to varied flora and fauna (Burgess et al., 2007). In Taita Hills, there are three main forest fragments; Chawia (86 ha), Mbololo (185 ha) and Ngangao (120 ha) and a number of other small fragments (Pellikka et al., 2009). These forest fragments are greatly disturbed by human activities. For instance, a large extent of exotic forest was lost in 2010 when the western side of Ngangao forest was set ablaze by human.

Forest mapping in Kenya has been limited to either indigenous or exotic level. At species level, only tedious and time consuming methods have been employed for identification of trees especially in the tropics. The development of sensors with high spectral resolution have offered new possibilities of forests mapping at species level by use of remote sensing techniques. These

techniques offer quick, up-to-date and accurate methods of discriminating between various tree species (Peerbhay et al., 2013).

There are various disadvantages of high spectral resolution of hyperspectral data (Dalponte et al., 2012; Jusoff and Pathan, 2009). Firstly, there's a strong correlation between bands. This can cause convergence instability in the classification of images and adversely affect the accuracy of classification. The classification accuracy will reduce if all the spectral bands are used in classification without any form of band selection. Several methods of waveband selection have been developed and applied. Some of them include: Stepwise Discriminant Analysis (SDA) (Clark et al., 2005), Principal Component Analysis (PCA), Random Forest (RF) (Mutanga et al., 2012), Maximum Likelihood Classification method (Jia and Richards, 1994). To overcome the shortcoming high dimensionality if hyperspectral data, a Stepwise Discriminant Analysis (SDA) should be used. For selection of suitable spectral bands for discrimination of various species, an appropriate method of the band selection should be applied. Secondly, there has to be adequate training samples to derive good classification results. Optimal spectral bands for classification are difficult to determine with inadequate training samples. Thirdly, the high number of spectral bands increases the image processing time and cost. Since hyperspectral data is rich in spectral information, it is important to evaluate and select optimal features for a concrete application target in order to accurately and effectively extract them from the image (Jusoff and Pathan, 2009).

1.2 Problem Statement

The indigenous tree species have been at risk of extinction and for this reason, it is necessary to quantify them in order to be able to manage and conserve them. In Kenya, forest management using remote sensing techniques has been widely driven by multispectral data such as Landsat and SPOT. However, use of hyperspectral data extends the scope of forest management to include species mapping, forest health, canopy structure and possibly forest ecosystem function analysis. The high spatial and spectral resolutions of hyperspectral data have made this possible. The existing methods of species identification are tedious and time consuming (Voss and Sugumaran, 2008). In addition, some parts of the forest are inaccessible and remote sensing techniques allow the tree species in these areas to be identified and mapped.

Figure 1.1 shows the locations where most of the studies on tree species mapping using remote sensing have been conducted throughout the world. These locations comprise temperate forest ecosystem (North America) and boreal forest (Europe), and very little in tropical forest (Central America) (Fassnacht et al., 2016). Fassnacht et al. (2016) further notes that the few studies conducted in Africa were in South Africa and focused mainly on savannah ecosystems. This shows that there is need to investigate the possibility of mapping tree species in the tropics and especially in the East Africa.

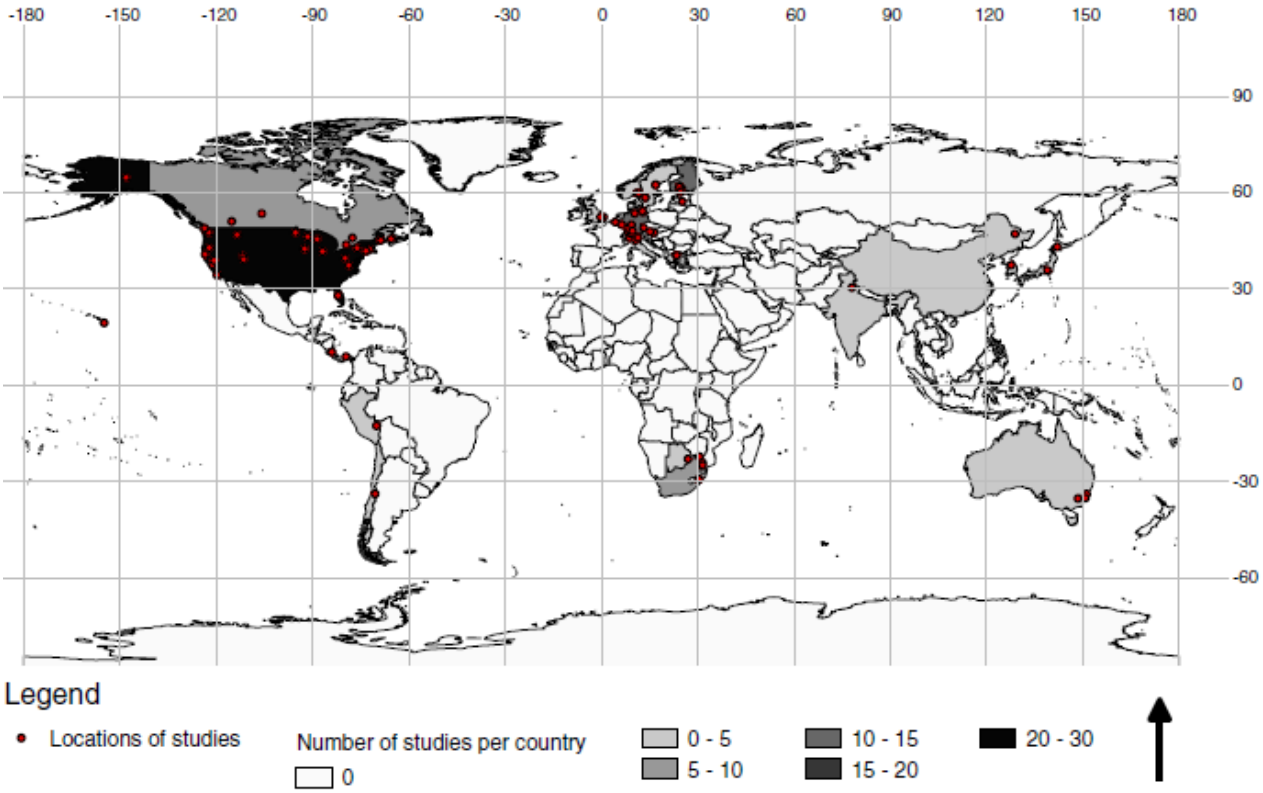

Figure 1.1: World map displaying locations where tree species mapping studies have been conducted throughout the world (red dots) (Fassnacht et al., 2016)

1.3 Objectives

The main objective of this research was to map indigenous and exotic tree species appearing on the top canopy from airborne hyperspectral data using Ngangao Forest as a case study.

The specific objectives were namely to:

i. Determine the appropriate wavelengths for mapping of selected tree species in Ngangao Forest.
ii. Map selected tree species using different classification algorithms and selected appropriate spectral bands from hyperspectral data in Ngangao Forest.
iii. Examine the potential application of simulated multispectral data in discriminating tree species in Ngangao Forest.

1.4 Justification for the Study

Trees contribute to sound environmental health by conservation and provision of water, provision of oxygen, purification of air, amelioration of climate, preservation of soil, and conservation of wildlife. Rain-fed agriculture is the main source of livelihood in Taita Hills. Forests, being an important driver to climate change, require optimal management for sustainable agricultural production. Ngangao Forest is rich in biodiversity. However, deforestation is evident in the forest through logging and forest fires, e.g. during the data collection, there was evidence of a section of forest that had burnt down. Salminen, (2004) notes that of all the forests in the Eastern Arc Mountains, Taita Hills has undergone the worst natural forest loss in the last 2000 years. Pellikka et al., (2009) reported that about half of the cloud forests in the hills were cleared for agricultural purposes between 1955 and 2004. Deforestation is said to reduce vapour flows derived from forests by 5% annually (Gordon et al., 2005). It is therefore important to quantify the forest cover and the constitution of the forest as different species contribute to the biodiversity of Ngangao Forest. Carbon storage vary with tree species and as a results, the outputs of this research could be used to model carbon sequestration in Taita Hills for subsequent projects.

Dalponte et al., (2012) notes that mapping of tree species is key to the development policies relating to forest conservation and management. Kenya Forest Service and Kenya Wildlife Service, who are the core managers of forests and forests ecosystems could significantly benefit from this study. Information on tree species distribution over a large area is also key to the understanding of ecology of tree species such as the contribution of the different species to the ecosystem functions and services. Ngangao Forest is home to endemic birds and tree species. National Museums of Kenya is concerned with the conservation of the biological diversity of the

East African region and this study could help them understand and manage the ecosystem of these endemic species.

There is no documented research on the use hyperspectral technology to identify tree species in East Africa. This research provides an alternative and faster approach in tree species identification in this region. Further, this research will justify why institutions and researchers may require to invest in hyperspectral technologies as compared to cheaper options of multispectral data in tree species identification. Different algorithms have been used in this research to map tree species. This research will advise on which of these algorithms are applicable in mapping of tree species using hyperspectral and multispectral data.

1.5 Scope of Work

The area of interest in this research is Ngangao Forest, which is one of the few remaining forest fragments in Taita Hills in south western Kenya. Ngangao Forest is reach in biodiversity and consists of a variety of tree species (Omoro et al., 2010). This research only focused on identifying 10 tree species (6 indigenous and 4 exotic species) whose crowns appear on the top canopy and were clearly visible on the aerial images. In addition, samples of these species were clearly identified in the field during field data collection.

The research examined techniques and algorithms that could facilitate the identification of tree species in tropical forests. The development of new algorithms is beyond the scope of this research. However, the research examined the utility of existing algorithms of mapping individual tree crowns and tree species using hyperspectral data and multispectral data. The multispectral data were simulated from hyperspectral data as opposed to the actual acquisition of these images. The hyperspectral data could not be calibrated using Analytical Spectral Devices (ASD) field spectrometers since the tree canopies could not be reached from the ground.

1.6 Organization of the thesis

This thesis is organized into six chapters. Chapter one gives the background of the study highlighting the importance of forests, forests ecosystems and species mapping. It further outlines the objectives of the research together with a justification of this study.

Chapter two generally examines the documented literature on hyperspectral data, multispectral data and the different algorithms of image processing and analysis. Various methods of reducing spectral redundancy in hyperspectral images and image classification algorithms have been explored. A number of case studies relating to forest mapping have been mention. Various approaches of assessing the accuracies of image classification have been highlighted.

Chapter three expounds on the methods that have been applied to achieve the objectives of this research. A comparison of the different band selection methods and tree species mapping algorithms has also been outlined. The area of study is also explained. Resampling of the hyperspectral data into two selected multispectral data for purposes of testing the possibility of using the later to map the tree species has been described.

Chapter four outlines the findings of this research based on the objectives of the study. Tree species mapping accuracies using the different algorithms and at different spatial and spectral resolutions have been given and explained. Chapter five gives critical discussions of the results achieved in this study.

Finally, chapter six draws the conclusions and the recommendations of this study. Areas of further research have been identified and the contribution the research to knowledge has also been outlined.

CHAPTER TWO
HYPERSPECTRAL DATA, MULTISPECTRAL DATA, AND IMAGE PROCESSING ALGORITHMS FOR TREE SPECIES MAPPING

There has been consistent increase in the mean global temperatures since the 1850s due to the increasing greenhouse gases in the atmosphere. The later has been caused by, (i) the burning of fossil fuels such as coal, oil and gas, to meet the growing demand for energy and (ii) the spread of intensive agricultural practices to meet the growing demand for food, which is often associated with deforestation. The increasing global temperatures shows no indications of waning and is expected to bring about long-term changes in the global climatic conditions (Hallegatte, 2009).

These changes will consequently bring severe impacts on the four aspects of food security, namely; food availability, food accessibility, food utilization and food system stability. The consequences are already being felt in global food markets, and are likely to be particularly significant in many rural areas where crops fail and yields significantly reduce. The impacts will be felt in both rural and urban areas where supply chains are interrupted, market prices rise, assets and livelihood opportunities are lost, purchasing power declines, human health is threatened, and affected people are unable to able to handle worsening conditions (Al et al., 2008; Godfray et al., 2010).

Concerns for the implications and consequences of adverse climate change have stimulated a considerable amount of research. Vegetation mapping, (including tree species mapping) is an essential task in management of natural resources as vegetation provides an ecosystem for all living creatures and plays an significant role in contributing to global climate change, such as influencing the terrestrial carbon dioxide (Xiao and Boyd, 2004). Xiao and Boyd (2004) further notes that classification and mapping of vegetation presents critical information in understanding both natural and man-made habitats through quantification of vegetation cover from local to universal levels at a specific time stamp or over a continuous time period. For purposes of initiating programs to support vegetation protection and rehabilitation it is critical to obtain current status of vegetation cover (Egbert and Erofeeva, 2002).

Traditional methods of mapping vegetation, (e.g. ground surveys, map interpretation reviews of existing literature and collateral and ancillary data analysis), are usually very costly and time consuming. Remote sensing technology provides economical and practical means to study vegetation cover changes, especially in large areas (Langley et al., 2001; Nordberg and Evertson, 2003). Remote sensing also provides data archives that can be made available to researchers for use over several decades. For instance, in 1992, the International Geosphere–Biosphere Program initiated a program to map global land cover in order to develop a Global Land Cover Characterization (GLCC) Database that was based on Advanced Very High Resolution Radiometer (AVHRR) of 1-km spatial resolution (DeFries et al., 1995; Vazquez et al., 1998). Similarly, in 1999, the Joint Research Institute of Italy in collaboration with over 30 research teams from around the globe implemented a similar project referred to as the Global Land Cover 2000 (GLC2000) to map land cover for the whole earth and consequently developed the VEGA2000 dataset using the SPOT4-VEGETATION imagery of 1-km spatial resolution (Bartholomé and Belward, 2005). Between January and December 2001, the National Aeronautics and Space Administration (NASA) of the United States developed a global MODIS land cover database based on monthly composites based on Levels 2 and 3 of the Terra MODIS data (Clark et al., 2010; Spruce et al., 2011). The approaches used in the development of the above land cover products together with the strengths and weaknesses of each of the approach were highlighted by Jung and Casler (2006).

For over half a century ago, aerial and satellite imagery of different spectral resolutions with wavelengths stretching from visible to microwave and with spatial resolutions ranging from a few centimetres to a few kilometres and with temporal resolutions running from half hour to months have been acquired. The main factors to consider when selecting images from different sensors include: (i) the objective of the mapping assignment, (ii) the cost of images, (iii) the climatic conditions at the time of capture and (iv) the technical issues related to image interpretation.

2.1 Pre-processing of Images for Tree Species Mapping

Image pre-processing includes (i) geometric correction to correct for geometric distortion due to sensor-Earth geometry and other imaging conditions, (ii) radiometric correction to correct for uneven sensor response over the whole image, and (iii) orthorectification to correct for the effects

of image perspective and relief for the purpose of creating a planimetrically correct image. Image pre-processing commonly comprises operations which include and not limited to replacement of bad lines and patches, geometric correction, radiometric correction, image enhancement and masking of water and clouds.

Prior to mapping of vegetation, pre-processing of satellite images is critical in order to remove or minimise noise resulting from the characteristics of the imaging system and imaging conditions. This initial processing will enhance the quality and the interpretability of image datasets. This is particularly the case when use of a time series imagery is made or when an area is covered by several images since it is fundamentally significant to make these images spatially and spectrally compatible. The pre-processed images should seem as if they have been captured by the same sensor after pre-processing (Toutin, 2004).

2.2 Vegetation Indices

A Vegetation Index (VI) refers to mathematical combination or transformation of spectral bands that emphasizes the spectral properties of green plants so that they appear distinct from other image features. Vegetation indices (VIs) are used to estimate the likelihood that vegetation was actively growing at the time of data acquisition. VIs are associated with canopy characteristics such as biomass, leaf area index, moisture content and percentage of vegetation cover. Table 2.1 shows some of commonly used Vegetation Indices as captured from literature.

Table 2.1: Commonly used Vegetation Indices, their formulae and characteristics.

Index	**Formula**	**Characteristics**	**Reference**
Atmospherically Resistant Vegetation Index (ARVI)	$\frac{NIR - RB}{NIR + RB}$ where $RB = R - \gamma(B - R)$	Has dynamic range to the NDVI. It has resistance to atmospheric effects	Kaufman and Tanre, 1992
Enhanced Vegetation Index (EVI)	$EVI = G\ X \frac{\rho_{NIR} - \rho_{Red}}{\rho_{NIR} + (C_1 X \rho_{Red} - C_2 X \rho_{Blue}) + L}$ where L is a soil adjustment factor, and C_1 and C_2 are coefficients used to correct aerosol scattering in the red band by the use of the blue band.	It has improved resistance to the atmosphere and less evidence of saturation at high Leaf Area Index (LAI).	Roberts et al., 2016; Matsushita, 2007
Normalized Difference Vegetation Index (NDVI)	$\frac{NIR - R}{NIR + R}$	It indicates the greenness level of vegetation and very useful is determining the health of vegetation.	Matsushita et al., 2007; Bannari, et al., 1995
Simple Ratio (SR)	$SR = \frac{NIR}{Red}$ Shows the amount of vegetation and reduces effects of atmosphere and topography	It depicts high values for vegetation and low for soil, ice, water, etc. It indicates amount of vegetation.	Roberts et al., 2016

Sum Green Index (SGI)	10 to 25 percent of the reflectance	Highly sensitive to small changes in vegetation canopy opening.	Lobell and Asner, 2003
Water Band Index (WBI)	$WBI = \frac{\rho_{970}}{\rho_{900}}$	It is a reflectance that is sensitive to changes in canopy water status.Water Band Index contrast liquid water absorption.	Roberts et al., 2016
Plant Senescence Reflectance Index (PSRI)	$\text{PSRI} = \frac{Red_{660} - Green_{510}}{NIR_{760}}$	It is sensitive to the senescence phase of plant development.	Hatfield and Prueger, 2010
Carotenoid Reflectance Index (CRI)	$CR = \frac{1}{\rho_{510}} - \frac{1}{\rho_{550}}$	It is a measure of stress in vegetation. Higher CRI values mean greater carotenoid concentration relative to chlorophyll.	Roberts et al., 2016
Anthocyanin Reflectance Index (ARI)	$ARI = \frac{1}{\rho_{550}} - \frac{1}{\rho_{700}}$	It uses reflectances in the green and red edge spectral bands to detect higher concentrations of anthocyanins in vegetation.	Roberts et al., 2016

Photochemical Reflectance Index (PRI)	$PRI = \frac{\rho_{531} - \rho_{570}}{\rho_{531} + \rho_{570}}$	It is a reflectance measurement that is sensitive to changes in carotenoid pigments (particularly xanthophyll pigments) in live foliage. It is used in studies of vegetation productivity and stress.	Roberts et al., 2016
Structure Insensitive Pigment Index (SIPI)	$SIPI = \frac{\rho_{800} - \rho_{445}}{\rho_{800} - \rho_{680}}$	It maximizes sensitivity to the ratio of bulk carotenoids to chlorophyll while minimizing the impact of the variable canopy structure. It is very useful in areas with high variability in the canopy structure, or leaf area index.	Roberts et al., 2016
Red Edge Normalized Difference Vegetation Index (RENDVI)	$RENDVI = \frac{\rho_{750} - \rho_{705}}{\rho_{750} + \rho_{705}}$	It capitalizes on the sensitivity of the vegetation red edge to small changes in canopy foliage content, gap fraction, and senescence.	Roberts et al., 2016

Vogelmann Red Edge Index 1 (VOG-1)	$VRE = \frac{\rho_{740}}{\rho_{720}}$	It is a narrowband reflectance measurement that is sensitive to the combined effects of foliage chlorophyll concentration, canopy leaf area, and water content.	Roberts et al., 2016
Visible Atmospherically Resistant Index (VARI)	$VARI = \frac{Green - Red}{Green + Red - Blue}$	It's used to estimate the fraction of vegetation in a scene with low sensitivity to atmospheric effects.	Roberts et al., 2016

2.3 Image Classification

Classification of an image entails the process of extracting differentiated classes or themes (e.g. land use categories and vegetation species) from raw remotely sensed data. The resulting classified image comprises of a mosaic of pixels, each of which belong to a particular these, and basically a thematic map of the raw image. This description also includes the pre-processing of the acquired images.

2.3.1 Traditional Image Classification Methods

The traditional methods of image classification employ the conventional algorithms, such as the K-mean and ISODATA for unsupervised image classification or the Maximum Likelihood Classification (MLC) for supervised image classification. In most cases, the unsupervised classification algorithms are used in thematic mapping, e.g. classification of vegetation from image data. These algorithms are usually easily applicable and are also widely available in most of the image pre-processing, analysis and statistical algorithms (Langley et al., 2001). The K-mean and the ISODATA clustering algorithms involve iterative procedures. The steps followed by both of the algorithms include: (i) assigning an arbitrary initial cluster vector, (ii) classification of each pixel to the closest cluster and, (iii) calculation of the new cluster mean vectors based on all the specific pixels in each of the clusters is executed. Steps (ii) and (iii) are repeated until the gap between the iteration is smaller than a pre-set threshold. The main difference between the two unsupervised classification algorithms is that the number of clusters do not change during the process of classification using K-means algorithm while the ISODATA algorithm removes the redundant clusters and creates new clusters, e.g. whenever a cluster centre is not assigned enough samples, it may be removed.

Unsupervised classification methods essentially depend on statistics which are spectrally pixel-based and in addition, they do not incorporate any prior knowledge of the characteristics of the classes or themes being investigated. The main advantage of applying unsupervised classification algorithms is to automatically convert raw image data into more meaningful information provided higher classification accuracies are achieved (Tso and Olsen, 2005). Alternatively, rather than relying on purely spectrally pixel-based, Tso and Olsen (2005) built a fundamental framework for unsupervised classification referred to as Hidden Markov Models (HMM) by incorporating both

spectral and contextual information. HMM showed significant improvements in both classification accuracies and visual qualities of the image. Duda and Canty (2002) investigated and compared unsupervised classification algorithms with respect to their capabilities to replicate field data in a multifaceted area. Notwithstanding its easy application, unsupervised classification has a disadvantage that the process of classification has to be repeated again and again if different training areas are incorporated.

Contrary to unsupervised classification, supervised classification algorithms performs classification based on training samples, that contain prediction variables estimated in each sampling unit and assigns prior information classes to the sampling units (Černá and Chytrý, 2005). Supervised classification assigns information classes to the rest of the pixels in the image. This means that, additional new data has no influence on the established standards of classification once the classifier has been set up, unlike the unsupervised classification. Maximum Likelihood Classification is based on the statistical distribution pattern; and usually regarded as a classic and most popular supervised classification algorithm for remote sensing images (Sohn and Rebello, 2002; Xu and Wunsch, 2005). MLC has the disadvantage that it assumes the data follows a Gaussian distribution which may not be the case especially in complex areas; and this leads to less satisfactory classification results. In addition, it is computationally intensive and also very slow.

2.3.2 Improved Image Classification Methods

In many occasions, the same vegetation type on the ground may have distinct spectral characteristics in remotely sensed imagery. Alternatively, it is common that different vegetation types may possess similar spectral characteristics, which makes it very difficult to obtain good classification results by using either the traditional unsupervised classification or supervised classification. Identification of desirable classification algorithms has always been a big challenge for remote sensing analysts. Nevertheless, all image classification algorithms are derived from the traditional classification algorithms as aforementioned. The later provide the basic principles and techniques for the classification of an image. Thus, improved methods usually rely on and expand on specific techniques or spectral features, which can lead to improved classification results and thus deserve special mention. In the recent past, commendable progress has been made in the development of more powerful image classification algorithms to extract vegetation covers from

remotely sensed images. A relevant example is Stuart et al. (2006), who developed continuous classifications using Landsat imagery to distinguish variations within Neotropical savannas and to discriminate between savanna areas, the associated gallery forests, seasonally dry forests and wetland communities. The results of this study showed that continuous classifications were better than MLC classification and especially in complex land cover areas.

In order to improve the classification accuracy, extensive field knowledge and auxiliary data such as elevation, soil types, weather parameters, etc. may be required. Gad and Kusky (2006) and Shrestha and Zinck, (2001) have shown that classification accuracy can significantly be improved by incorporating expert knowledge and ancillary data in the extraction of thematic features such as vegetation types. At a larger scale, Domaç and Süzen (2006) incorporated vegetation-related environmental variables in the image classification conducted in the Amanos Mountains region of southern central Turkey using Landsat images, and considerably improved classification accuracy when compared with the traditional MLC classification. Under many circumstances, however, gathering specific knowledge is a massive task and collection of ancillary data is very expensive and time consuming. For these reasons, the knowledge-based classification algorithms are not commonly used.

Sohn and Rebello (2002) developed supervised and unsupervised Spectral Angle Classifiers (SAC), which normally take into consideration that the spectral characteristics of the same type of surface objects are approximately linearly scaled variations of one another as a result of the topographic and atmospheric effects of the environment. Those SAC helped identify the distances between pairs of signatures for classification and were successfully applied in biotic community and land cover classification (Sohn and Qi, 2005). The adoption of Vegetation Indices (VIs) including the most widely and commonly used Normalized Difference Vegetation Index (NDVI) and its optimized form, Enhanced Vegetation Index (EVI), is another method to map vegetation using optical sensors (DeFries et al., 1995). These VIs could also be incorporated in the classification as additional variables. The main principle of applying NDVI in mapping of vegetation cover is that vegetation is highly reflective and absorptive in the near infrared and in the visible red of the Electromagnetic Spectrum (EM) respectively. The contrast between these channels of EM can be used as an indicator of the status and types of the vegetation. In other word,

NDVI is a biophysical characteristic that correlates with photosynthetic process of vegetation. In addition to providing an indication of the vegetation greenness, NDVI is also able to offer valuable information of the dynamic changes of specific vegetation species given that multiple-time images are analysed (Wang and Tenhunen, 2004). Consequently, NDVI is a good indicator to reflect periodically dynamic changes of vegetation types (Geerken et al., 2005). Particular vegetation categories can be identified through their unique phenology, or dynamic signals of NDVI (Lenney et al., 1996), which is also referred to as 'Multi-temporal Image Classification'. Another approach to identify specific vegetation groups is to study time series VIs. An example of this is that Bagan et al. (2005) applied the combined EVI multi-dataset generated from 16-day interval Moderate Resolution Imaging Spectroradiometer (MODIS) data during the growing season of plants as input parameters to match the features of vegetation types and to classify the images. The achieved results of classification were compared with those of the traditional MLC algorithm and the accuracy of the former exceeded that of the latter.

Artificial Neural Network (ANN) and Fuzzy Logic classification approaches for vegetation discrimination have also been applied and reported in literature. ANN is applicable for the analysis of almost all kinds of imagery without regard to their statistical properties. Filippi and Jensen (2006) reports that ANN is very useful in extraction of vegetation-type information in complex vegetation mapping problems. However, this is usually at the expense of the interpretability of the results since ANN deploys a black-box approach that hides the underlying prediction process (Černá and Chytrý, 2005). Berberoglu et al. (2000) achieved an accuracy of 15% higher than the accuracy achieved using a standard per-pixel MLC algorithm by combining ANN and texture analysis on a per-field basis to classify land cover. However, one major drawback of ANN is that it is usually computationally demanding when large datasets are used to train the network and sometimes it may return no results even after running the computation for a while due to the local minimum especially for the backpropagation ANN.

The fuzzy classification approach is usually useful where there is evidence of mixed-class areas. It has been investigated for the classification of suburban land cover from remote sensing imagery, the study of medium (10years)-to-long term (50 years) vegetation changes (Okeke and Karnieli, 2006) and the biotic-based grassland classification (Xie et al., 2008). Fuzzy classification method

is more of a probability-based classification as opposed to crisp classification. Unlike implementing per-pixel-based classifier to produce crisp or hard classification, Xu et al. (2005) employed a Decision Tree (DT) derived from the regression approach to determine class proportions within a pixel so as to produce a soft classification. Theoretically, probability-based or soft classification is more reasonable for composite units since those units cannot be simply classified to one type but to a probability for that type. While soft classification techniques are inherently appealing for mapping vegetation transition, there is an unresolved issue of how best to present the output. Rather than imposing subjective boundaries on the end-member communities, transition zones of intermediate vegetation classes between the end-member communities were adopted to better represent the softened classification result (Xie et al., 2008).

Decision Tree (DT) approach is another method of vegetation classification by matching the spectral features or combinations of spectral features from images with those of possible end-members of vegetation types (species or family level). As compared to ANN, DT is computationally less intensive, makes no statistical assumptions and can handle data that are represented on different measurement scales. A global land cover map deduced from AVHRR imagery was produced by Hansen et al. (2006) using a DT that has a set of 41 metrics generated from five spectral channels and NDVI for input. The agreements for all classes varied from an average of 65% when viewing all pixels to an average of 82% when viewing only those 1 km pixels consisting of >90% one class within the high-resolution datasets. Other studies integrated soft classification with DT approach (Xu and Wunsch, 2005). Pal and Mather (2003) studied the utility of DT classifiers for land cover classification using multispectral and hyperspectral data and compared the performance of the DT classifier with that of the ANN and ML classifiers, with changes in training data size, choice of attribute selection measures, pruning methods and boosting. They found that the use of DT classifiers with high-dimensional (hyperspectral data) is limited while good results were achieved with multispectral data. Under some circumstances, DT can be very useful when vegetation types are strictly associated with other natural conditions (e.g. soil type or topography) (Egbert and Erofeeva, 2002). For example, some vegetation species may only grow in areas with elevation higher than a certain level. This can be integrated within DT to assist the classification process from imagery if such ancillary data are available.

2.4 Data Dimensionality Reduction

Data dimensionality is a big challenge when dealing with hyperspectral data. It requires more processing power apportionment, more storage space and handling the data is complex. Dimensionality reduction provides the ability to handle data more easily. Image transformation techniques typically use statistical analysis to reduce the dimensionality of the data. There are several procedures that can be employed for dimensionality reduction in hyperspectral data analysis. They include Minimum Noise Fraction (MNF) transformation, Pixel Purity Index (PPI), is especially important in identifying extreme or spectrally pure pixels, the n Dimensional Visualizer for determining the endmember directly from the image and Random Forest for identifying the fractional data contribution of each band to the species reflectance.

MNF is important in the reduction of the inherent dataset dimensionality and noise. The data computational requirement is reduced after application of MNF (Denghui and Le, 2011), and decorrelates and rescales noise in datasets. MNF transforms data that has noise with unit variance to data that has no band to band interrelationship. Thereafter, it performs the independent component analysis for data that has been cleaned/whitened of noise (Chen and Kovacevic, 2003) to produce much smaller spectral angles than those derived in transformed space (Mundt et al., 2005). In practice, 95% of the information is contained in the first ten inverse MNF bands. PPI aims at finding the most spectrally pure/extreme pixels in image data (Chang and Plaza, 2006) which correspond to mixing endmembers.

N-Dimensional Visualization is applied after correcting the image. Where 'N' is the number of bands, the coordinates of the bands in 'N' space consisting of 'N' values that are simply the spectral radiance and reflectance values in each band of a given spectrum and reflectance values in each band of a given pixel. The distribution of bands in 'N 'space can be used for estimation of some spectral endmembers and their pure spectral signature. The 'N' dimensional visualization is applied after gathering the data through MNF or PPI algorithms. Since the purest pixel is to find in the neighbourhood of the data cloud, the n-Dimensional visualizer allows for interactive rotation of data in n-D space, selection of group into different classes (Boardman& Kruse, 1999). Of all the dimensionality reduction methods, Random Forest performs best because it ranks variables according to their importance based on the out of box error.

2.5 Variable Selection

Random Forest ranks variables based on their importance by randomly permuting variables associated with the 'out-of-bag' (OOB) samples and growing regression trees on the modified dataset (Breiman, 2001). If the original variables are associated with the response variables, then the Mean Square Error (MSE) will substantially decrease. Therefore, to measure the importance of the variables in the final random forest model, the MSE difference before and after permuting the variables is used. Besides dealing with the impact of each variables individually, random forest also assesses the interactions with other variables (Strobl and Zeileis, 2008).

Recursive backward propagation method was used by the "varSe1RF" package (Diaz-Uriarte and Diaz-Uriarte, 2010) in the R statistical software (R. Core Team, 2014) to select the smallest possible subset of the important AISA Eagle spectral bands with required information that would achieve comparable classification accuracy. RF returned the importance of each band (n=129) using the OOB as the selection criteria. While eliminating the least important spectral bands, multiple RF models were repeatedly built from the training data, while building a new RF model each round. A .632+ bootstrap (n=10) method with replacement (Efron and Tibshirani, 1997) was employed at each loop in order to aggressively reduce the bands subspace without any over-fitting while evaluating the selection procedure (Abdel-Rahman et al., 2015). The .632+ bootstrapping employs the leave-one-out cross-validation procedure from the subspace not used in the classification model fitting (Diaz-Uriarte and Diaz-Uriarte, 2010). The subset with the smallest number of spectral bands and lowest OOB error estimate after termination of the loops was chosen as the optimal for the classification process. Collinearity between selected AISA Eagle bands was tested using a Pearson correlation test since predictor variable selection using such methods have been shown to be highly correlated in previous studies (Deng and Runger, 2012).

2.6 Hyperspectral Imagery and Data Fusion for Vegetation Mapping

Hyperspectral imagery and multiple imagery fusion have been used recently to extract vegetation cover and thus deserve special attention and further investigation. Xie et al. (2008) noted that more advanced methods reflecting the latest remote sensing techniques used in vegetation mapping have been documented in recent past.

2.6.1 Vegetation Mapping from Hyperspectral Imagery

Recently, there has been an increase in the use of hyperspectral imagery for vegetation extraction as compared to the use multispectral imagery that only has a few spectral bands; hyperspectral imagery includes hundreds of spectral bands (Xie et al., 2008). Hyperspectral sensors are well suited for mapping of vegetation as the ability of the individual species or mixed communities of the species to reflect or absorb active or passive light can well be examined from the much wider spectral bands of hyperspectral data (Varshney and Arora, 2004). The hyperspectral imagery from Airborne Visible Infrared Imaging Spectrometer (AVIRIS) has commonly been used in the remote sensing studies of the earth surface. AVIRIS is a special optical sensor which acquires calibrated images with spectral resolution of 224 contiguous spectral bands and wavelength ranging from 400 to 2500 nm. The information contained in these spectral bands can be exploited to detect, measure and monitor the components of the surface of the earth based on molecular absorption and scattering signatures. A case in particular is where AVIRIS imagery was used to classify salt marshes in China and in San Pablo Bay of California, USA (Li et al., 2005). The results of this study were acceptable considering the success in identifying two main marsh vegetation species (i.e. Spartina and Salicornia), which covered 94% of the total mash vegetation. However, more research work was recommended to correct the false detection of other marsh vegetation species. Xie et al. (2008) conducted similar work to study the structure of wetlands in San Francisco Bay of California by monitoring vegetation dynamics for purposes of recommending sustainable management of wetland ecosystems. In Brazil, discrimination of five important Brazilian sugarcane varieties was evaluated by use of hyperspectral data acquired by the Hyperion sensor on board the Earth Observing-1 (EO-1) satellite (Galvao et al., 2005). The results of this study illustrated revealed that the five Brazilian sugarcane varieties were discriminated using the Hyperion data. This was evidence that hyperspectral imagery is capable of discriminating between plant species, which may be very difficult by using multispectral images.

While the pre-processing and classification procedures of hyperspectral images are similar to those of multispectral images, the processing of hyperspectral imagery poses a great challenge because of the hundreds of spectral bands. For this reason, specialized, cost effective and computationally efficient image processing procedures are required (Varshney and Arora, 2004). A set of signature libraries of vegetation are usually required in order to discriminate between different vegetation

communities or species using hyperspectral imagery (Xie et al., 2008). The vegetation libraries for certain vegetation communities or species might be readily available for certain applications. For most cases, however, the spectral signature library is usually established using field spectrometers or the ground truthing data with hyperspectral data. Therefore, mapping of vegetation mapping by use of hyperspectral data has to be deigned well in order to collect synchronous field data for creating imagery signatures for classification.

2.6.2 Vegetation Mapping Through Image Fusion

The information extracted from images from a single sensor may be inconsistent, inadequate and imprecise for a specific application. In order to improve the accuracy and quality of vegetation classification, fusion of remotely sensed image data with different spatial resolutions is an effective method that can be employed. It is essential for accurate mapping of vegetation to efficiently integrate remotely sensed information with different spatial, spectral and temporal resolutions through image fusion. There are several studies that have been conducted aimed at the development of new image fusion algorithms (Amarsaikhan and Douglas, 2004; Zhu and Tateishi, 2006). To illustrate this, Elith et al. (2006) studied the fusion of high spatial resolution panchromatic and low spatial resolution multispectral remotely sensed images and proposed a frequency buffer model to overcome the challenge of detecting high-frequency components of panchromatic images and low frequency components of multispectral images. Another example was illustrated by Zhu and Tateishi (2006) who developed a new temporal fusion classification model to study land cover classification and verified its improved performance over the conventional methods based on the statistical fusion of multi-temporal satellite images. Behnia (2005) also compared four frequently adopted algorithms of image fusion, namely brovey transform, principle component transform, smoothing filter-based intensity modulation and hue–saturation–value (HIS) transform and established that each of the algorithms effectively improves the spatial resolution but distorts the original spectral signatures to certain extent (Behnia, 2005). In order to address the colour distortion problem associated with some existing techniques, Wu et al. (2005) developed normalized algorithm for colour enhancement to merge lower spatial resolution multispectral images with a higher spatial resolution panchromatic image (Wu et al., 2005). Instead of developing new fusion algorithms, Colditz et al. (2006) tested various existing methods of image fusion to study their impacts on the accuracies of land cover classification

ranging from simple and common algorithms such as brovey transform, HSI transform and principal component analysis to more complex approaches such as wavelet transformation, adaptive image fusion and multi-sensor multi-resolution image fusion algorithms. As discussed above, it is noted that image fusion opens a new way of extracting high accuracy vegetation covers by integrating remotely sensed images captured by different sensors, though the challenges of fusion strategy (including developing new algorithms of image fusion) still require more research.

2.7 Results Evaluation of Vegetation Mapping from Remote Sensing

The products of vegetation mapping derived from remote sensed images should be objectively verified and communicated to users so that they can make informed decisions on whether and how the products can be used. Result evaluation, a procedure also called accuracy assessment, is often employed to determine the degree of 'correctness' of the classified vegetation groups compared to the actual ones. A vegetation map derived from image classification is considered accurate if it provides a true representation of the region it portrays (Foody, 2002) (Weber, 2006). Four significant stages have been witnessed in accuracy assessment methods (Congalton, 1994). Accuracy assessment in the first stage was done by visual inspection of derived maps. This method is deemed to be highly subjective and often not accurate. The second stage used a more objective method by which comparisons of the area extents of the classes in the derived thematic maps (e.g. the percentage of a specific vegetation group in area) were made with the corresponding extents on ground or in other reference dataset. However, there is a major problem with this non-site-specific approach since the correct proportions of vegetation groups do not necessarily mean the correct locations. In the third stage, the accuracy metrics were built on a comparison of the class labels in the thematic map with the ground data for the same locations. Measures such as the percentages of cases correctly (and wrongly) classified were used to evaluate the classification accuracy. The accuracy assessment at the fourth stage made further refinements on the basis of the third stage. The obvious characteristic of this stage is the wide use of the confusion or error matrix, which describes the fitness between the derived classes and the reference data through using measures like overall accuracy and kappa coefficient. Additionally, a variety of other measures are also available or can be derived from the error matrix. For example, the accuracy of individual classes can be derived if the user is interested in specific vegetation groups.

Although it is agreed that accuracy assessment is important to qualify the result of image classification, it is probably impossible to specify a single, all-purpose measure for assessing classification accuracy. For example, the confusion matrix and its derived measures of accuracy may seem reasonable and feasible. However, they may not be applicable under some circumstances, especially in vegetation mapping at coarse scales (Cingolani et al., 2004). One of the problems caused by the pixel-based confusion matrix evaluation is that a pixel at a coarse resolution may include several vegetation types. As represented by Figure 2.1, a pixel in an imagery represents a composite of three vegetation classes (class A, B and C). Clearly, the ellipse located at the centre of the pixel may be the sampling area. Since it is impractical to sample the whole pixel at a large-scale mapping, this pixel would most likely be labelled with class B in image classification considering its percentage of the occupied area. Therefore, the vegetation class between the derived (class B) and the referenced (class A) will not match and this mismatch will introduce classification errors. In this case, the non-site-specific accuracy measures may be more suitable if not for the limitation mentioned previously. Moreover, rather than using field samples to test the classification accuracy, a widely accepted practice is to use finer resolution satellite data to assess coarser resolution products (Cihlar et al., 2003), although the high-resolution data are themselves subject to interpretation and possible errors (DeFries et al., 1999). The result evaluating for image classification still remains a hot debating topic today (Foody, 2002).

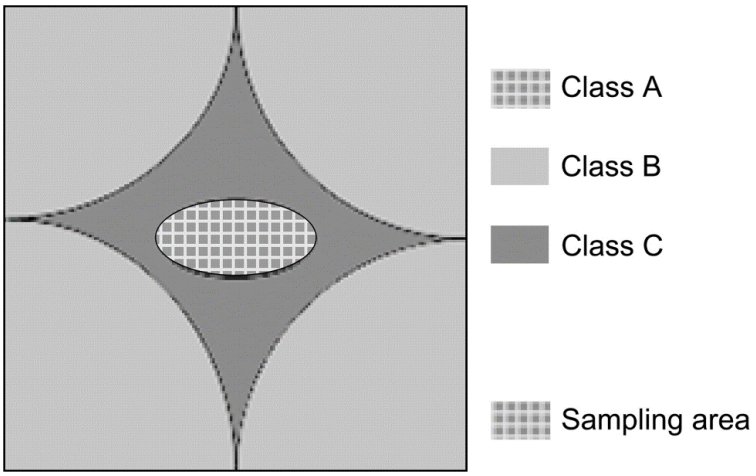

Figure 2.1: An illustration of a pixel-based accuracy assessment of a coarse spatial resolution (Xie et al., 2008)

CHAPTER THREE
METHODOLOGY

3.1 Study Area

Ngangao forest (38°20’E, 03°21’S) is one of the few forest fragments remaining in Taita Hills, Kenya. The Taita Hills are located at approximately 100 km east of Kilimanjaro and 175 km from the Kenyan coast (Figure 3.1). The area is known for bimodal pattern of rainfall with long rains occurring between March and May and the short rains between November and December, but the hilltops receive mist and cloud precipitation throughout the year (Pellikka et al., 2009; Rogers et al., 2008). Pellikka et al. (2005) notes that the average rainfall at and around the hills is approximately 1500 mm. Ngangao forest is located on an eastern slope of a north–south oriented mountain ridge with the western slope mainly covered by open rock and some patches of *Acacia mearnsii* and *Pinus patula* plantations. The forest is managed by the Kenya Forest Service and covers an area of about approximately hectares with the elevation ranging from 1700–1952 m above mean sea level (Omoro et al., 2010). The forest is rich in biodiversity, with many indigenous trees, bird species and patches of exotic tree species.

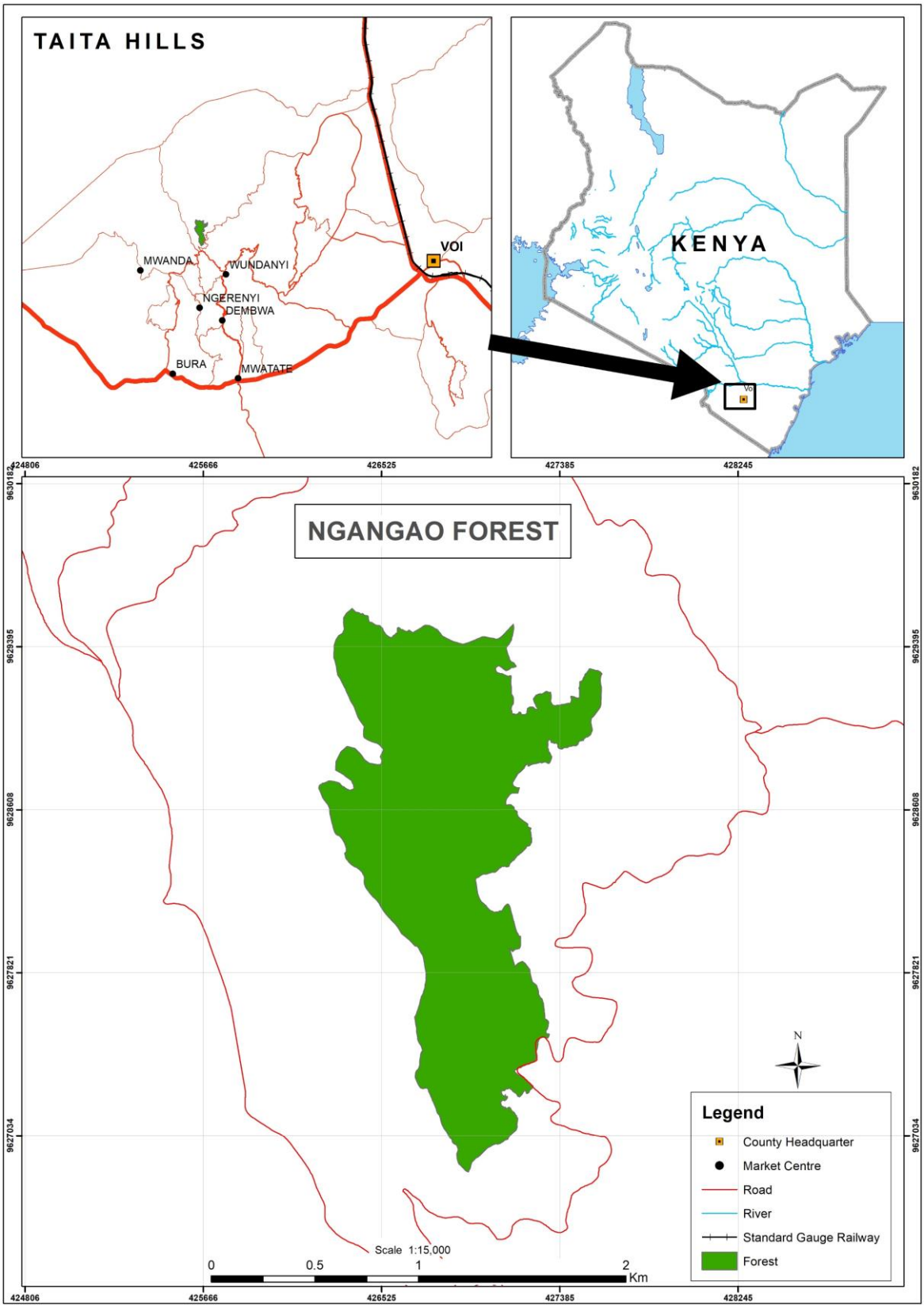

Figure 3.1: Location of the study area (Ngangao Forest).

3.1.1 Demographics and Livelihood in Taita Hills

Taita Hills is dominated by subtribe of Taita people called Wadawida and the local language is Dawida. The population has been growing rapidly from 108,000 people in 1969 to 280,000 in 2009 (KNBS, 2010) with most of this population concentrated on the highlands. The increasing population has exerted pressure on the forests and people depend on these forests for firewood, grazing and crop production. As earlier reported in this thesis, Pellikka et al. (2009) notes that approximately 50% of cloud forest was cleared for purposes of agricultural production between the years 1955 and 2004, and currently about 1% of the original indigenous forest area is remaining. During the field work, there was evidence of farming activities encroaching into parts of the eastern side of Ngangao forest. This is as a result of increasing population.

Small scale agriculture is the main source of livelihood in Taita Hills (Pellikka et al., 2009), with different crops being grown at different elevations (Salminen, 2004). There are two main planting seasons as dictated by the rainfall patterns. Low-lying uplands, plains and low-lands are intensively cropped with cereals, tuber and horticultural crops. Agroforestry is also practised in the highlands and mid-lands. Livestock farming is also practised in small scale due to small farm sizes and grazing areas; especially in the highlands where the climatic conditions are favourable. The people around the forests often graze on the edges and sometimes inside. Charcoal burning is also practised in the lowlands. Other sources of livelihood as observed during the field work include retail shops, sand harvesting, mining, bee keeping and tourism.

3.1.2 Climate

Taita Hills receives bi-modal type of rainfall with long rains and short rains occurring between March and May and November and December respectively. The rainfall amounts average between 1332 – 1910 mm per annum (Salminen, 2004). The southern and eastern slopes of Taita Hills receive more rainfall than western and northern slopes (Omoro et al., 2013) with some parts, especially the highlands, receiving cloud precipitation (Jaetzold, 1983). At the same time, the air can contain more humidity as temperatures increase with decreasing elevation. Most of the tropical forest fragments in the Taita Hills are found in the highlands and therefore the forest influence the rainfall amounts and distributions.

3.2 Acquisition and Pre-Processing of Hyperspectral Images

The hyperspectral imagery used in this study was acquired on 4th February 2013 by use of an Airborne Imaging Spectrometer for Applications (AISA) Eagle VNIR sensor at an average flying height of about 2300 m above the mean sea level. This is usually a dry season with low cloud cover in many parts of Kenya including Taita Hills. The spectral range of the AISA sensor is 400 to 1000 nm and was processed to 129 spectral bands which had bandwidth of about 4.6 nm. A total of 11 flight lines running along the West-East direction with swath width of about 500 m covered the entire of the Ngangao Forest.

The acquired images were then corrected for radiometric and atmospheric effects by means of CaliGeo Pro and ATCOR-4 software, respectively. A 20 m spatial resolution Digital Elevation Model (DEM) was resampled to 1 m spatial resolution and used for the orthorectification of the images. ENVI software was then used to correct for the geometric effects of the atmospherically corrected images by use of the Geographic Lookup Table (GLT) files generated by the CaliGeo Pro software.

3.3 Definition of Training Areas

High spatial resolution aerial photographs, which were acquired during the January 2012 flight campaign using Nikon D3X digital camera were used in the field to delineate the selected tree crowns only (Figure 3.3). No significant difference was expected with the one-year difference between the acquisition of hyperspectral data and the aerial photographs. These delineated tree crowns could be identified both on the photographs and on the ground. The crowns were randomly sampled and identified in the field mainly from the top of the open rocks, footpaths within the forest and along the edges of the forest (Figure 3.2). The plantation patches within Ngangao Forest were easily identified and training areas delineated.

Figure 3.2: A section of Ngangao Forest as viewed from one of the highest points in the forest. (Researcher, 2013).

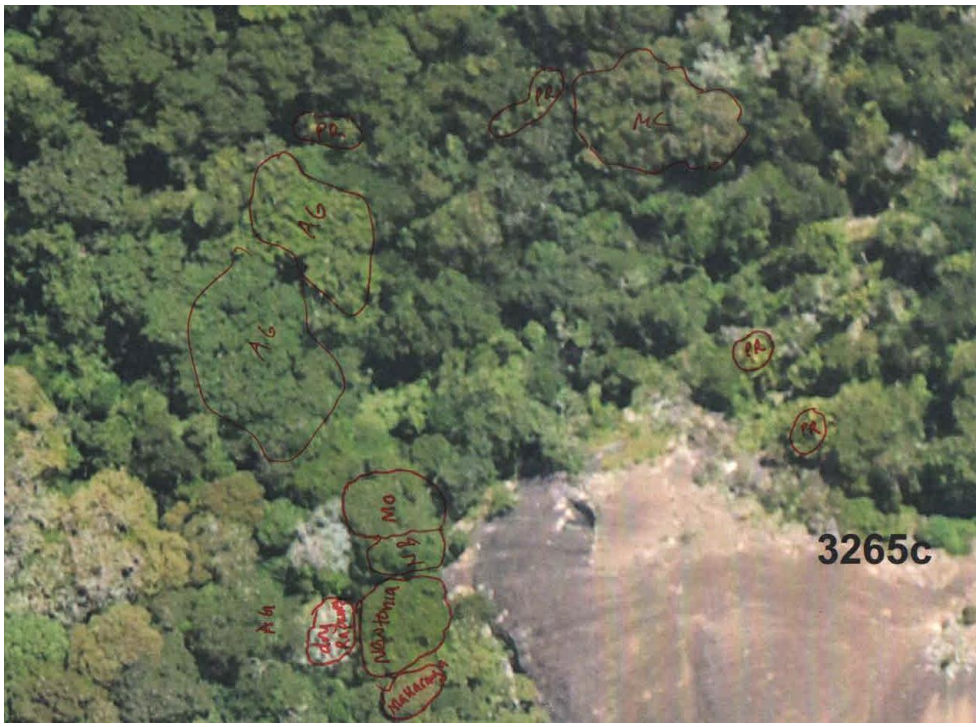

Figure 3.3: An illustration of delineated tree crowns that were identified both on the ground and on the aerial photographs.

The delineated crowns on the photographs were then identified and on-screen digitized from the true colour composites of the hyperspectral images using ArcGIS 10 software (Figure 3.4)

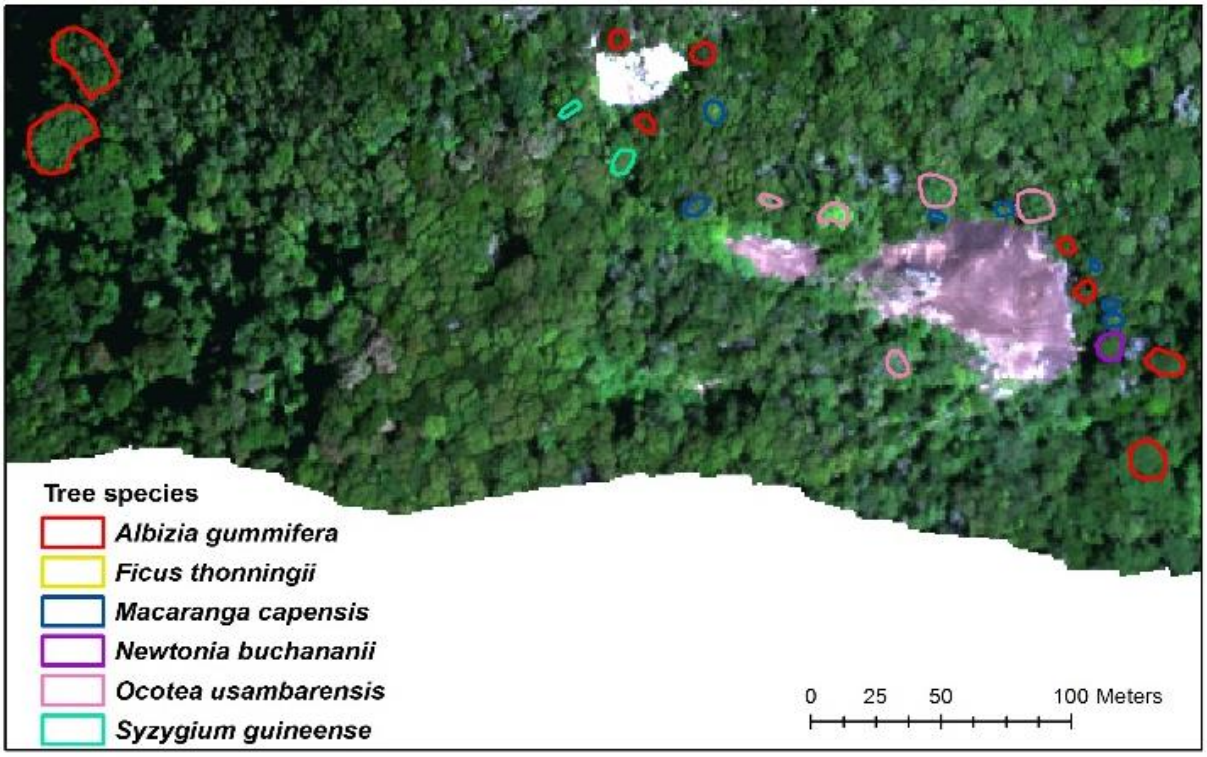

Figure 3.4: A section of a true colour composite AISA Eagle image overlaid with delineated tree crown polygons.

Since the flight campaign was conducted in the mid-morning hours of the day, some of tree crowns were partly covered by shadows and therefore only the sun-lit parts of the tree crowns were digitized. The exotic species usually have smaller crowns as compared to indigenous species and the former are mostly plantation patches of the forest. For this reason, small sections of the plantation forest were identified and digitized to represent the training data for the specified species. All tree species with identifiable pure endmembers were sampled, totalling to 152 samples, which were digitized representing 10 different tree species (6 indigenous and 4 exotic species) (Table 3.1). Some of the commonly found indigenous tree species in Ngangao forest are *albizia gummifera*, *ficus thonningii* and *newtonia buchananii*, while those of exotic species are *acacia mearnsii*, *cupressus lusitanica* and *pinus patula*.

The mean spectral reflectance of each of the tree crowns was extracted from the AISA Eagle image for each of the processed 129 bands. Consequently, the mean spectral reflectance of each tree species was then computed. However, wavelengths ranging from 876 to1000 nm were not used in the analysis as they exhibited spectral noise and were therefore not used in the analysis. As a result, 103 of 129 spectral bands were used in the subsequent analysis. The mean spectral reflectance curves of both the indigenous and exotic tree species respectively are represented by Figures 3.5 and 3.6.

Table 3.1: Indigenous and Exotic tree species studied and their respective number of samples (n).

Name of Species (scientific name)	**Family name**	**Local name (Dawida)**	**Type**	***n***
Acacia mearnsii	*Fabaceae*	Mgamu	Exotic	11
Cupressus lusitanica	*Cupressaceae*	Musumbesu	Exotic	10
Eucalyptus spp.	*Myrtaceae*	Mkongo	Exotic	21
Pinus patula	*Pinaceae*	Mubunduki	Exotic	29
Albizia gummifera	*Mimosaceae*	Msuruwachi	Indigenous	37
Ficus thonningii	*Moraceae*	Muvumu	Indigenous	10
Macaranga capensis	*Euphorbiaceae*	Shao	Indigenous	14
Newtonia buchananii	*Mimosaceae*	Chamsidu	Indigenous	7
Ocotea usambarensis	*Lauraceae*	Manyoda	Indigenous	5
Syzygium guineense	*Myrtaceae*	Mzambarau	Indigenous	8
Total				**152**

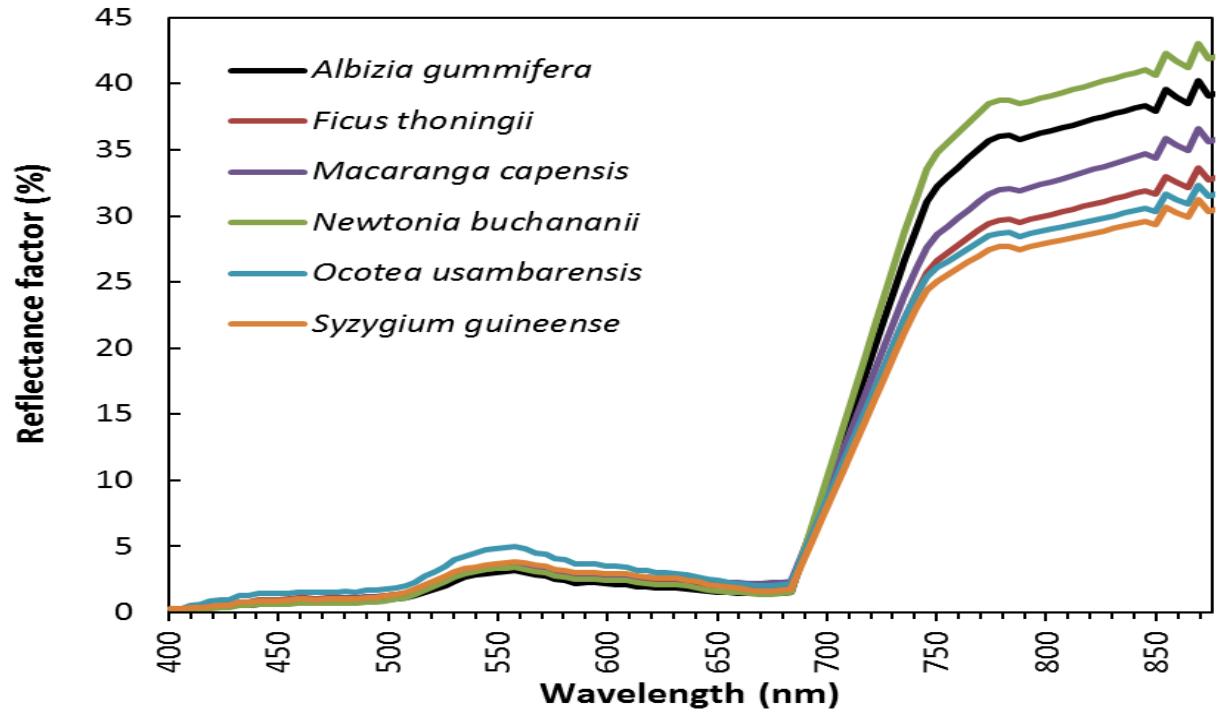

Figure 3.5: Spectral reflectance curves corresponding to the indigenous tree species.

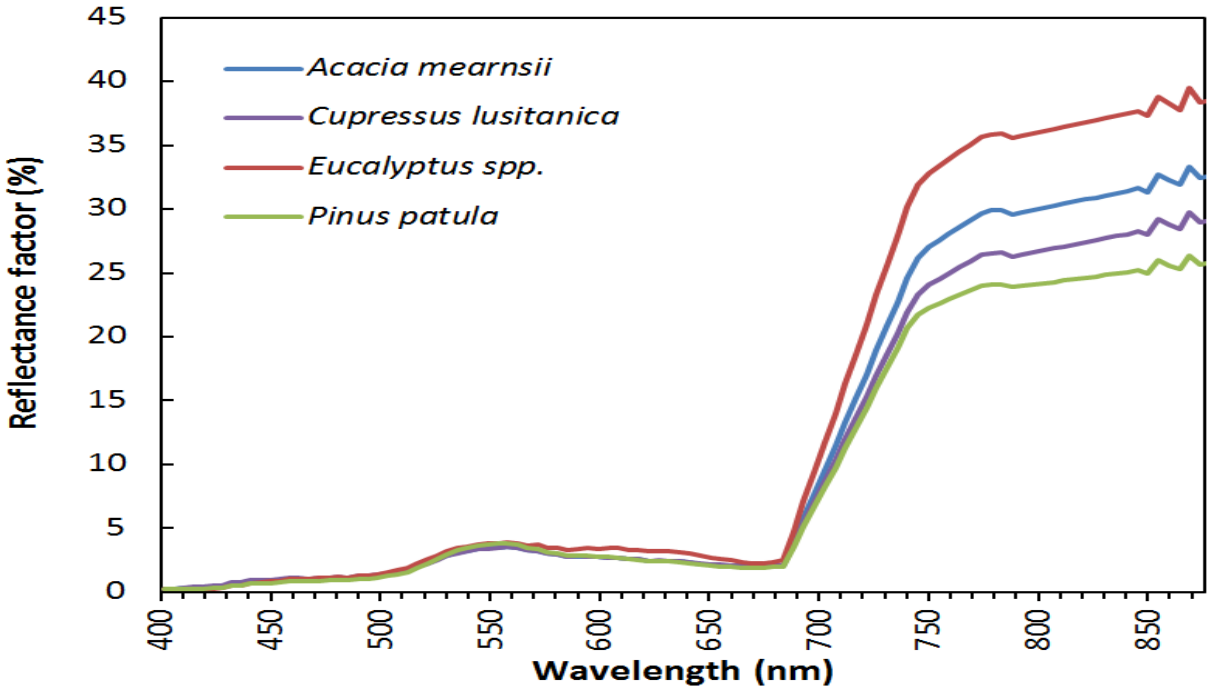

Figure 3.6: Spectral reflectance curves corresponding to the exotic tree species.

3.4 Narrow band Vegetation Indices

A number of Vegetation Indices (VIs) can be calculated from hyperspectral imagery and applied in tree species discrimination. In this study, the following indices were computed: Atmospherically Resistant Vegetation Index (ARVI), Enhanced Vegetation Index (EVI), Normalized Difference Vegetation Index (NDVI), Simple Ratio (SR), Sum Green Index (SGI), Water Band Index (WBI), Plant Senescence Reflectance Index (PSRI), Carotenoid Reflectance Index (CRI), Anthocyanin Reflectance Index (ARI), Photochemical Reflectance Index (PRI), Structure Insensitive Pigment Index (SIPI), Red Edge Normalized Difference Vegetation Index (RENDVI), Vogelmann Red Edge Index 1 (VOG-1), Visible Atmospherically Resistant Index (VARI) and Visible Green Index (VIg). This led to a total of 128 variables which included 103 spectral bands and 15 computed VIs. The purpose of computing these vegetation indices was to increase the variables to be considered for the discrimination of the tree species. Different tree species will return different values of the VIs due to the unique physiological characteristics of different species.

Additionally, four distinct broadbands were computed as the average of the spectral reflectance of the respective wavelength ranges of the AISA spectral bands (Table 3.2).

Table 3.2: Simulated broadband wavelengths.

Broadband	**Wavelength range (nm)**	**No. of spectral bands**
Blue	0.42 – 0.52	16
Green	0.52 – 0.60	18
Red	0.63 – 0.69	13
Near Infra-Red	0.76 – 0.86	25

3.5 Statistical Analysis

The Stepwise Discriminant Analysis (SDA) provided by the Predictive Analytics Software (PASW) Statistics 18 application was used for statistical analysis and subsequent classification of the AISA Eagle data. In order to build the discriminant functions for each of the tree species studied, SDA uses the reflectance values from the training classes. (Clark et al., 2005).

SDA consists of a feature selection technique that reiterates the addition and removal of a certain feature at every single step of the analysis. This process enables one to find the best subset with

which suitable feature discrimination results can be realized. A linear function that relates the dependent variables (i.e. tree species) and the independent variables (i.e. spectral bands and VIs) was generated. At each stage of the discrimination, more variables were added on the function while the invaluable ones were removed. This process was repeated till none of the remaining variables appeared to further improve the classification accuracy. Evaluation of whether the variables were entered into or removed from the discriminant model was done using the Fischer statistic. Wilks' Lambda was used to measure the discriminatory power of the model while the leave-one-out cross validation method was used to validate classification results. Consequently, the samples of each tree species were classified by the linear function derived from all the samples besides the samples left out for validation.

3.6 Algorithms for Data Dimensionality Reduction and Mapping Selected Tree Species in Ngangao Forest

Hyperspectral images contain several hundreds of bands with spectra of fine spatial resolution stored in several wavelengths (Landgrebe, 1999). Every pixel contains proportionate values to the detailed spectrum of reflected light (Chang, 2003). Therefore, hyperspectral images have the ability to discriminate between hard to distinguish features in every spatial location, making it ideal for classification of heterogeneous classes such as species discrimination. Therefore, it is paramount to extract the right spectra and to choose the right classifier.

The dimensionality in hyperspectral data make them unique and feature extraction is done with caution. For instance, to avoid the Hughes phenomena (Hughes, 1968) of the dimensionality curse, one needs to collect more training samples than is required in multispectral images. The curse in dimensionality leads to overfitting of classification models whereby training samples provide a good fit while the classifier performs poorly in testing samples. A good classifier incorporates the landscape heterogeneity and is able to deal with the large volumes of data in hyperspectral datasets. More often than not, data is multi class and nonlinear in nature. Therefore, it is important to get enough training data from a wider scale of features in the image with accurate feature selection process (Kavitha and Arivazhagan, 2010).

Classification of hyperspectral data can either be spectral or spatial classification. This is based on the dimension which an algorithm uses to apportion the reflectance in the data. When the pixel reflectance values are considered at different wavelengths, the classification is considered spectral. This is because a pixel will exhibit different reflectance across the different wavebands or wavelengths in this dimension. Spectral features calculated/derived from the dimension of wavelength and reflectance include maximum reflectance, minimum reflectance, mean reflectance, variance and standard deviation. Identification and extraction of spatial arrangements and contextual values of pixels, and basing a classification on textural properties of an image among others is considered spatial classification. It is pixel based and each pixel is assigned a class depending on its spectral value (Tarabalka et al., 2009). There are various classification methods in this category, including decision trees (Goel et al., 2003; Zhou et al., 2005), maximum likelihood/Bayesian estimation methods (Landgrebe, 2005), genetic algorithms (Vaiphasa, 2003), genetic algorithms based methods (Hernández-Espinosa et al., 2004; Subramanian et al., 1997; Yang, 1999), kernel based techniques and Support Vector Machines (SVM) which produce good classification results with high dimensionality data with less training data or with Hughes phenomena (Camps-Valls and Bruzzone, 2005; Fauvel, 2007; Fauvel et al., 2006; Gualtieri and Cromp, 1999).

In classification, contextual information is as important as statistical information. The use of the neighbourhood of a pixel (Camps-Valls et al., 2006) improves classification than considering only conventional methods such as Spectral Angle Mapper (SAM). In literature, different authors have put forth the use of different methods, such as use of adaptive neighbourhood of each pixel (Fauvel et al., 2008), adaptive neighbourhood along with clustering information for segmentation-based classification (4) and kernel formulation by estimating wavelength decomposition of an image (Mercier and Girard-Ardhuin, 2006).

Within the framework the classifiers, spectral angle classifiers are among the earliest in hyperspectral image classification (Landgrebe, 1999). The reference spectra (spectral signature) play a major role as they provide a reference point from which the input image spectra can be compared. The calculation of angular separation between the spectral signature and the input image provide the basis for decision making on the placement of the pixel. The process is time

consuming and more often with poor accuracy. For this reason, machine learning algorithms such as SVM, Neural Network and Random Forest are important and can often distinguish between complex boundaries (Vapnik, 1998). The complex process run in the background and specifically SVM does not require much data pre-processing with more accurate outputs (Camps-Valls et al., 2006).

3.6.1 Spectral Angle Mapping

The Spectral Angle Mapping (SAM) algorithm is important in hyperspectral data correction. It belongs to the category of supervised image correction, where a pixel with minimum spectral angle comparison with reference spectra is assigned to the pixel vector. Spectral similarity between two pixels is determined by comparing the angles between them, which are then treated as vectors in space. Their dimensionality is equal to the number of bands in the data (Boardman, 1994; Sarhrouni et al., 2012). Pixels with least spectral angle dissimilarities are considered to be of the same class. Algorithm testing provide basis for calculating the angle between two spectra (van der Meer, 2006).

$$\alpha = \cos^{-1}\left(\frac{\sum_{i=1}^{nb} t_i r_i}{\left(\sum_{i=1}^{nb} t_i^2\right)^{1/2}\left(\sum_{i=1}^{nb} r_i^2\right)^{1/2}} \right)$$

Where nb = number of bands

t_i = test spectrum

r_i = reference spectrum (3.1)

3.6.2 Support Vector Machines

Support Vector Machine (SVM) algorithm has an advantage of outperforming other algorithms because it performs well with minimum training sites. It is non-linear and robust classification algorithm with kernel trick. SVM finds the separating hyper plane in some feature space inducted by the kernel function while all the computations are done in the original space itself (Vapnik, 1998). For the given training set, the decision function is determined by resolving the convex optimization problem.

3.6.3 Artificial Neural Networks

The Artificial Neural Networks (ANNs) borrow from the complexity of the human brain. This is because the human brain is very efficient at synthesising data from different sources (Atkinson and Tatnall, 1997). Therefore, the artificial neurons developed by mathematicians simulates this by developing algorithms to process vast amounts of data from different sources to unearth the complexities in datasets and make sense out of them, as Artificial Intelligence (AI). In classification, ANNs transforms data from feature space into class space, making them part of the automated pattern recognition technique (Ritter et al., 1988). This method is arguably one of the accurate and rapid method of classification available (Abraham, 2005; Benediktsson et al., 1997; Dayhoff and DeLeo, 2001; Goel et al., 2003; Yegnanarayana, 2009).

3.6.4 Random Forest Algorithm

The Random Forest (RF) (Breiman, 2001) ensemble allows for the growing, without statistical pruning, of many regression trees (*ntrees*), whose average gives the result. The trees in the forest are constructed by randomly drawing a bootstrap sample from the original training dataset (Breiman, 2001), with replacement (bootstrap aggregation/bagging). Each tree consists of two thirds (67%) bootstrapped randomly and independently subspace which are used for prediction, while one-third (33%) are excluded for testing (Prasad and Snyder, 2006). The two thirds part of the sample used for training is known as the 'in-bag' sample while one third part of the sample excluded for testing is termed as the 'out-of-bag' (OOB) instances (Breiman, 2001). From a subset of randomly selected features (*mtry*), tree nodes are split until all nodes have the same class (Liaw and Wiener, 2002). Afterwards, the results of all trees are combined by a majority vote (Breiman, 2001). When calculating the predictive accuracy of the model using Mean Square Error (MSE), the OOB samples provides an unbiased assessment given that they are not used in training (Pang et al., 2006; Prasad and Snyder, 2006). The MSE of the model can be estimated by aggregating the OOB predictions of all trees in the forest (Liaw and Wiener, 2002) as shown in Equation 3.2;

$$MSE^{OOB} = \frac{\sum_{i=1}^{n}(Y_i - \hat{Y}_i^{OOB})^2}{n} \quad (3.2)$$

where n represents the number of samples, Y_i represents the age of the forest and Y_i^{OOB} represents the mean of the OOB predictions for the i^{th} observation (Dye et al., 2011).

A random subset of the input variable establishes each tree split in addition to bagging (Breiman, 2001). Therefore random forest is an accurate tool for prediction due to the randomness in selection of the datasets (bagging) and variable selection (*mtry*) (Breiman, 2001; Liaw and Wiener, 2002; Peters et al., 2007). The number of trees grown (*ntrees*) and the number of possible splitting (*mtry*) sampled at each node (Ismail and Mutanga, 2010; Liaw and Wiener, 2002; Peters et al., 2007), are the only key parameters required in growing a random forest (Dye et al., 2011).
In this study, samples from different species were segregated into training data (70%) and testing data (30%) as shown in Table 3.3.

Table 3.3: Data from different tree species used in this study, (70% for training while 30% for validation).

Class	**Training**	**Validation**	**Total**
Acacia mearnsii	96	40	136
Albizia gummefera	189	80	269
Craibia zimmermannii	39	16	55
Ficus thoningii	243	104	347
Macaranga capensis	169	72	241
Newtonia buchananii	178	75	253
Ocotea usambarensis	157	66	223
Phoenix reclinata	49	20	69
Pinus patula	460	197	657
Syzygium guineense	178	76	254

A random sample of 30% of the reference data points from Table 3.3 was used to test the classification accuracy of using the Random Forest algorithm. Further, an error matrix of

classification results was generated to calculate the accuracy. The overall accuracy (OA), user's accuracy (UA) and producer's accuracy (PA), between reference test data and prediction (Cohen, 1960; Congalton and Green, 2008; Pontius and Millones, 2011) were calculated for all RF models. The McNemar's test was used to test whether there was a statistical significance between map accuracy using the entire AISA Eagle subspace and the reduced subspace after the variable selection. The results of the accuracy assessment are presented under the Results chapter.

3.7 Testing the Potential Application of Simulated Multispectral Data in Discriminating Tree Species in Taita Hills

Remote sensing of tree species identification assumes that each species has a unique spectral niche that is defined by the species biophysical and biochemical make-up (Asner and Martin, 2012; Cho et al., 2012; Clark et al., 2010). In theory therefore, it is possible to identify and separate every tree species using images obtained in the field. In this regard, a rich spectral library that provides the ability to divide the entire or part of the spectrum into separable units is paramount. However, mapping of trees species is hampered by low spectral resolution in multispectral images and the high cost of acquisition of hyperspectral images. Despite the cost, hyperspectral data is important in the determination of spectral separability between species when building a spectral library. The improved division of the electromagnetic spectrum in hyperspectral data gives narrow band data the ability to resolve subtle spectral canopy features such as carotenoid and chlorophyll content and foliar nutrients (Cho et al., 2012; Mitchell et al., 2012; Thulin et al., 2012).

In spite of the good characteristics about narrow band data, it has the disadvantage of high dimensionality, especially when using conventional classification techniques. The Hughes effect in hyperspectral data (Colgan et al., 2012; Rodríguez-Castañeda et al., 2012) and high redundancy rates of some bands (Sarhrouni et al., 2012; Yin et al., 2012) in particular applications is problematic. This is because a classifier's ability to generalize accurately is reduced (Beniwal and Arora, 2012; Chu et al., 2012) leading to the need for very large samples to achieve good description of data distribution (Dalponte et al., 2012). In addition, multicollinearity is experienced which is introduced by the use of highly correlated predictor variables (Makori et al., 2017; Numata et al., 2012). Multicollinearity becomes a challenge when discriminating between vegetation species with reflectance similarities in hyperspectral data (Ferwerda et al., 2005; Zhang

et al., 2011). Moreover, when the training data is insufficient, parameterization may not be reliable for feature selection (Chi and Bruzzone, 2007).

In such cases, working with scaled data or with few narrow bands become optimal for species discrimination while minimizing the headache of the curse of dimensionality (Cho et al., 2012). The physical or spectroscopic meaning of wave bands is analysed to identify important bands which are in turn resampled from the high-dimensional spectra to wider bandwidth intervals (Becker et al., 2007; Schmidt and Skidmore, 2003). There are operational multispectral sensors with few narrow bands such as Worldview 2 & 3, and Sentinel 2 (Hedley et al., 2012; Immitzer et al., 2012). They are designed to capture specific wavelengths such as the red-edge and yellow spectrum in addition to the wavelengths in the conventional multispectral images.

3.7.1 Worldview 2

Worldview 2 is a multispectral imaging sensor that was launched in the 2009 by DigitalGlobe. It acquires images with 8 spectral bands and a spatial resolution of 1.84 m & 0.5 m panchromatic band, with a spectral range from 400 nm to 1,050 nm (Immitzer et al., 2012; Padwick et al., 2010). The spectral bands range from coastal band, blue, green, yellow, red, red edge to the longer wavelength near infrared band. The wavelength range of the multispectral Wordview-2 Sensor is as represented in Table 3.4.

Table 3.4: Wavelength range and number of bands for scaled Worldview 2 used for classification.

S/No	Band	Wavelength range (nm)	No. of resample spectral bands
1	Coastal	400 – 450	12
2	Blue	450 – 510	13
3	Green	510 – 580	16
4	Yellow	585 – 625	10
5	Red	630 -690	15
6	Red Edge	705 – 745	10
7	Near-IR1	770 – 895	26
8	Near-IR2	860 – 1,040	30

The spectral response of individual bands is shown in Figure 3.7. The separation of individual spectral responses to map tree species indicate that it has a high potential in tree species mapping (Immitzer et al., 2012) with bands that are strongly related to vegetation. The yellow band is used to detect the senesce stage of vegetation, red-edge to discriminate heathy from unhealthy plants and vegetation age differences, and (Near Infra-Red) NIR 1 and 2 are mainly used for vegetation analysis since they are less affected by the atmosphere (Immitzer et al., 2012).

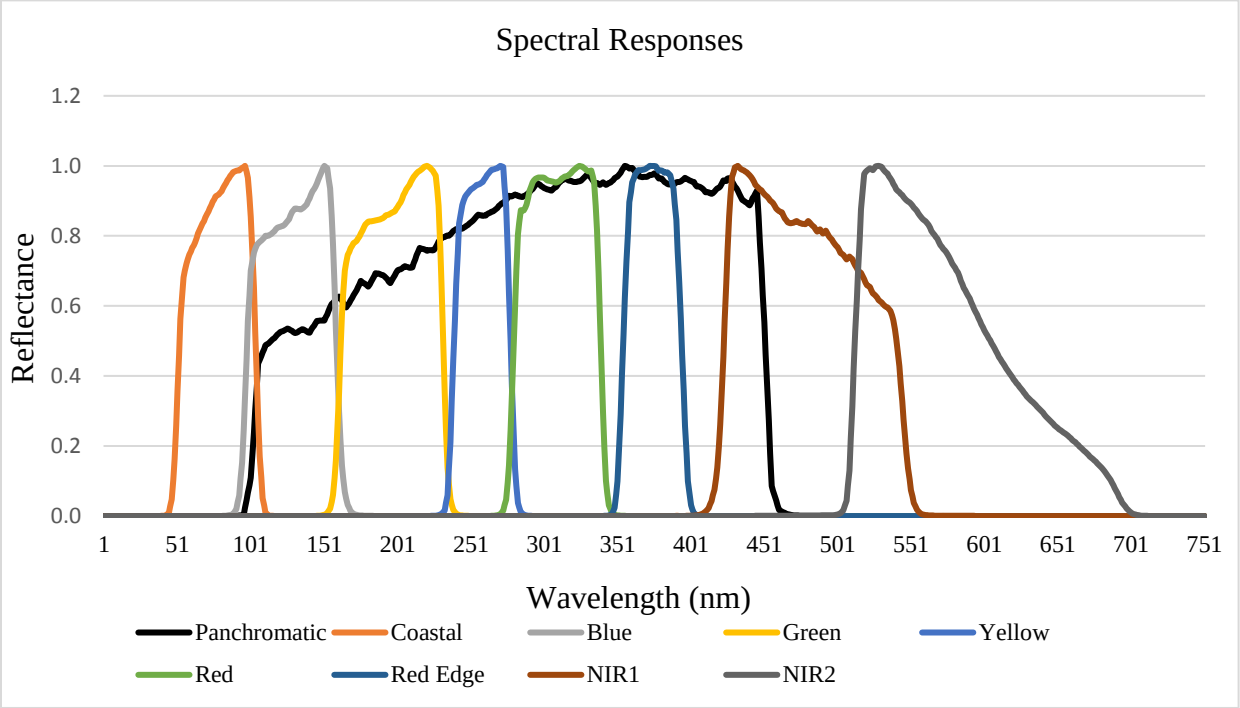

Figure 3.7: Spectral responses for the spectral bands found in Worldview 2.

Spectral configuration provides better identification of tree species. Worldview 2 has been shown to map big crown tree species with promising results e.g. (Cho et al., 2012; Colgan et al., 2012; Latif et al., 2012; Omar, 2010). However, studies in the coastal region of Kenya especially the Ngangao forest are still missing.

3.7.2 Sentinel 2

Sentinel 2 is an Earth observation mission developed by the European Space Agency (ESA) and was launched in June 2015. It acquires multispectral imagery with a spatial resolution of 10 metres and 13 spectral bands in the visible, near infrared and shortwave infrared ranges (Hedley et al.,

2012; Stratoulias et al., 2015; "User Guides - Sentinel-2 MSI - Sentinel Online," n.d., p. 2) (Table 3.5). It consists of two satellites (A and B) coupled to give a temporal resolution of 5 days. Its purpose is for land observation including soil, vegetation and water. It consists of several wavelengths that are important for vegetation mapping and species identification such as blue, green, red, red edge (which is divided into 4), Near Infra-Red (NIR) and Short-wave Infra-Red (SWIR) (Clasen et al., 2015; Immitzer et al., 2016; Stratoulias et al., 2015). The spectral responses of individual bands of the Sentinel 2 imagery that are within the range of the AISA Eagle sensor are shown in Figure 3.8.

Table 3.5: Wavelength range for Sentinel 2 resampled from AISA Eagle image.

Band number	**Centre λ nm**
B1	443
B2	490
B3	560
B4	665
B5	705
B6	740
B7	783
B8	842
B8a	865
B9	945
B10	1375
B11	1610
B12	2190

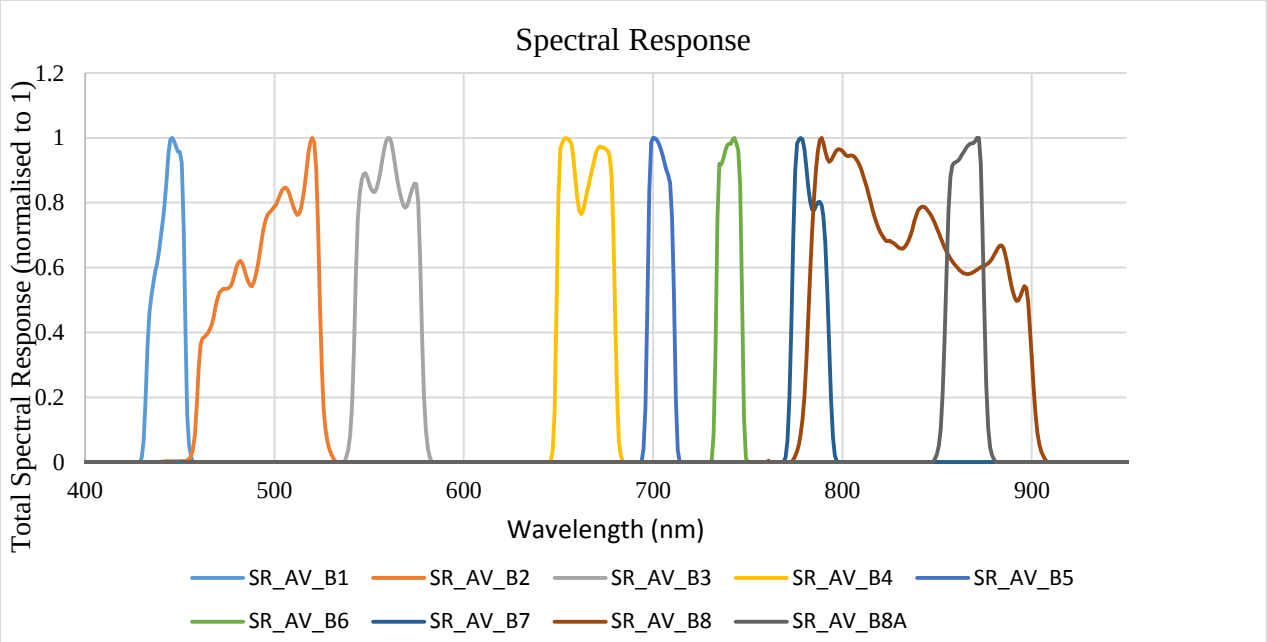

Figure 3.8: Spectral responses for the spectral bands found in Sentinel 2.

CHAPTER FOUR

RESULTS

4.1 Selection of Appropriate Spectral Bands for Mapping of Tree Species in Ngangao Forest

Different dimension reduction methods were used to select the optimal bands for the classification of tree species in Ngangao Forest. Independent Component Analysis (ICA) was set at above 1,000 Eigenvalues. This resulted in 32 optimal bands used in the classification. A plot of the endmember spectra of the selected bands indicated that the separability of the different classes (Figure 4.1 A) was not achieved well due to the transformations done by the ICA. Further, Principal Component Analysis (PCA) achieved better results in band reduction, achieving 13 bands from the 129 band image. But the endmember spectra indicated that most of the information was concentrated in the first and second bands of the image while the rest of the bands were rendered redundant (Figure 4.1 B). Therefore, species separability from this image was not achieved due to the similarity in species spectral resemblance after the third band. The same setting yielded 20 bands when using the Minimum Noise Fraction (MNF) algorithm (Figure 4.1 C). The separability between species was not pronounced enough to enable the classification of species to proceed. The random forest algorithm produced desirable results with the reduction of bands to 53 and good spectral separability.

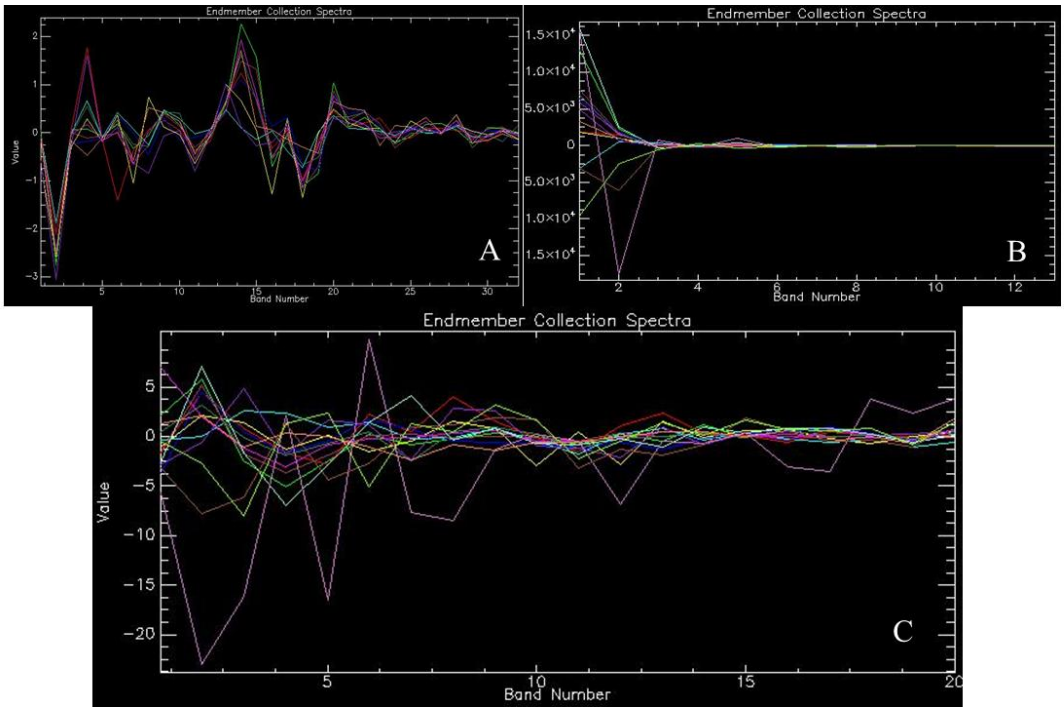

Figure 4.1: Band separation spectra for tree species mapping in Ngangao Forest in Taita Hills.

Figures 4.2 and 4.3 present the usefulness of AISA Eagle bands to map tree species in Ngangao Forest using RF. The selected bands are centred around the blue (400-500 nm), green (500-600 nm), red edge (650-690 nm) and in the infra-red (860-950 nm) regions of the Electromagnetic Spectrum (EMS) were the most important for discriminating amongst the different tree species than any other regions of the EMS. The OOB error rate changed with increasing number of spectral bands (*n*=129) using the .632+ bootstrap selection method. The result was a fewer number of bands (53) that accurately discriminated amongst the different tree species in Ngangao Forest with no significant decrease in mapping accuracy. Most of the important bands are found in the infrared and green regions of the EMS. The Pearson Correlation Coefficient (r) evidently showed that most of the spectral bands from the AISA Eagle (with 129 bands) were redundant and contained similar spectral information for mapping tree species in Ngangao Forest (Figure 3.4).

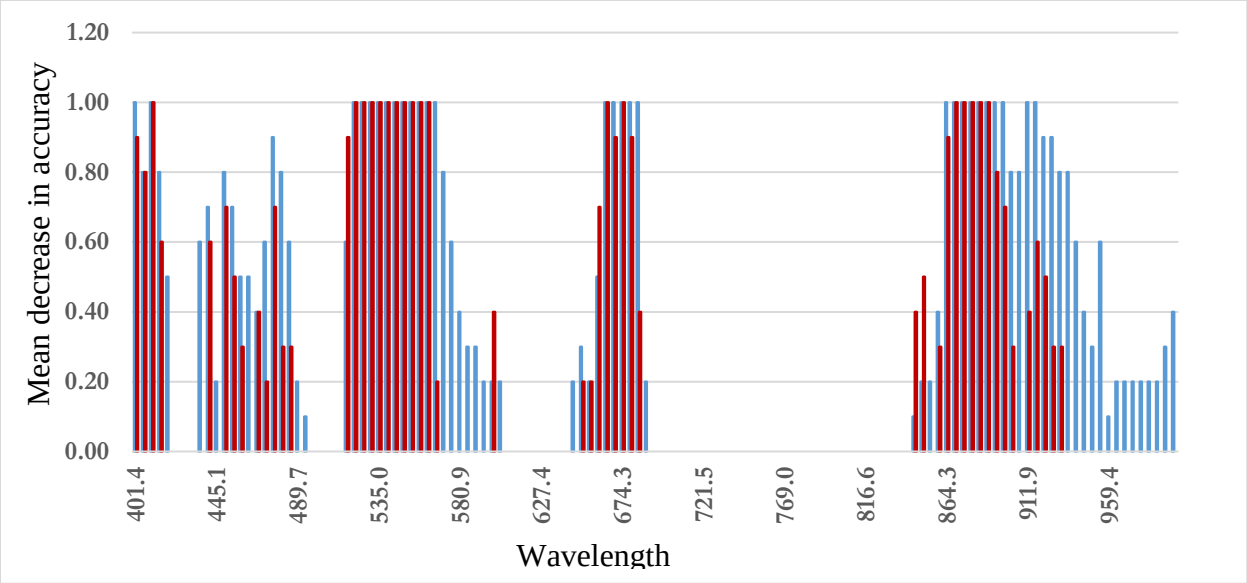

Figure 4.2: Usefulness of the AISA Eagle wavebands measured by the random forest classifier.

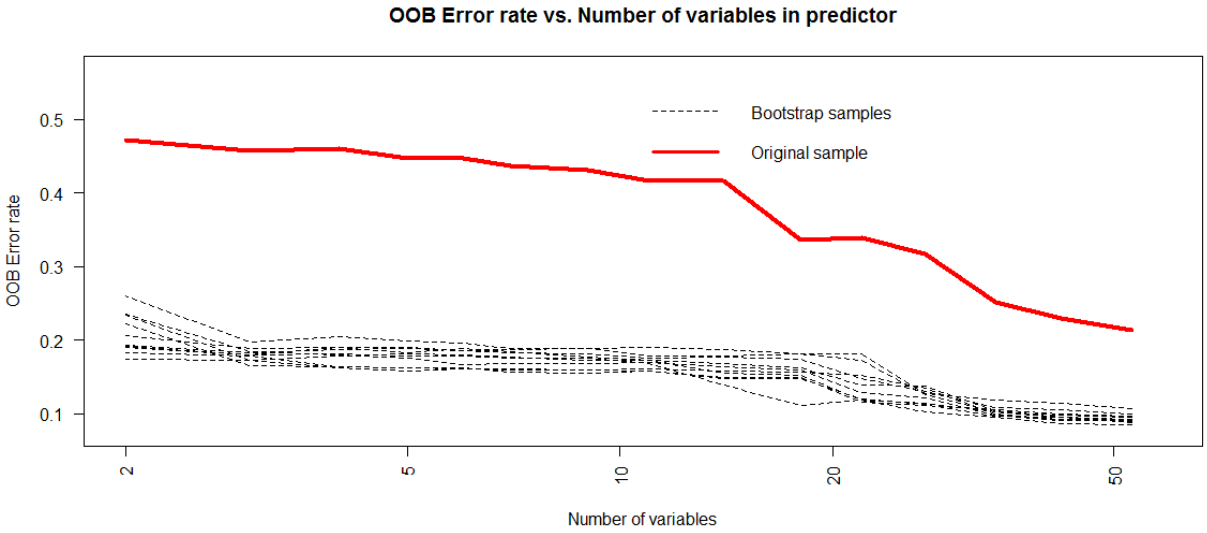

Figure 4.3: OOB error of backward selection and .632+ bootstrapping for wavebands importance.

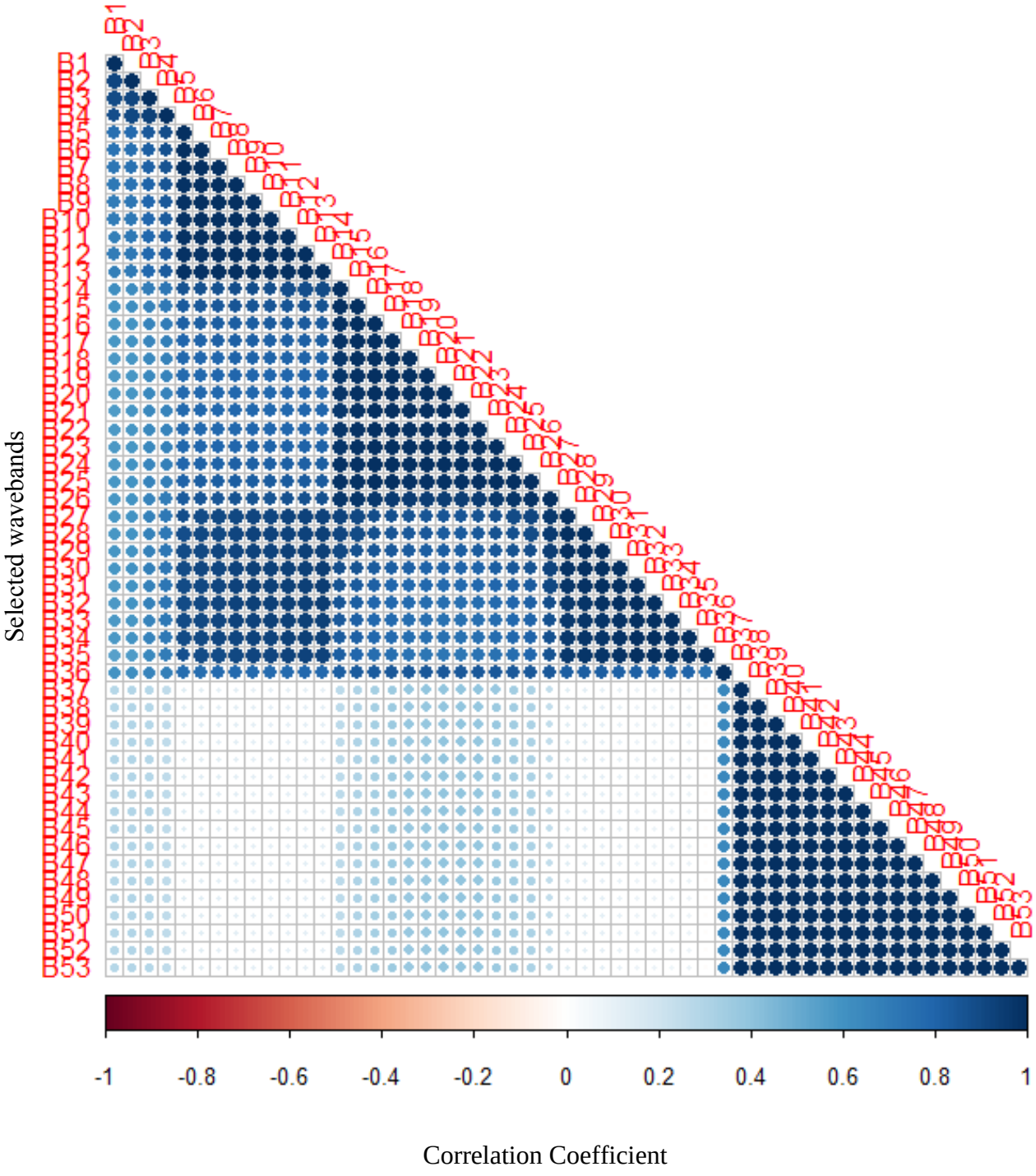

Figure 4.4: Correlation Coefficient (r) of the reflectance of wavebands of AISA Eagle.

4.2 Mapping Tree Species using Different Classification Algorithms and Selected Appropriate Spectral Bands in Ngangao Forest

All the four classification methods used to map tree species in Ngangao Forest were machine learning algorithms. They achieved varying accuracies ranging from 49% to 80% (Table 4.1). As presented in Table 4.1, the Spectral Angle Mapper achieved the lowest accuracy while Support Vector Machine and Random Forest achieved the highest accuracies. Random Forest ensemble has an advantage over Support Vector Machine since it considers many regression trees at the same time without statistical pruning and considers all bands in the image and ranks them according to the statistical importance. Therefore, Random Forest was preferred over the other classification methods.

Table 4.1: Comparison of the Classification Accuracies for Species Classification in Ngangao Forest.

		Neural Network		**Support Vector Machine**		**Spectral Angle Mapper**		**Random Forest**	
		P/A	U/A	P/A	U/A	P/A	U/A	P/A	U/A
1	*Albizia gummifera*	95.17	76.42	89.22	78.18	52.42	42.34	90.00	85.71
2	*Phoenix reclinata*	55.07	45.78	33.33	69.70	26.09	60.00	50.00	58.82
3	*Newtonia buchananii*	71.94	93.81	79.45	75.00	69.57	67.69	86.67	92.86
4	*Syzygium guineense*	71.26	69.35	74.80	72.52	39.76	33.44	64.47	77.78
5	*Pinus patula*	98.02	89.94	97.72	90.17	72.75	84.90	94.92	85.00
6	*Ficus thoningii*	77.23	72.63	71.76	80.58	27.38	49.48	86.54	76.27
7	*Macaranga capensis*	62.24	82.87	66.80	74.54	29.46	33.65	58.33	79.25
8	*Acacia mearnsii*	72.06	65.33	76.47	63.80	27.94	20.11	65.00	65.00
9	*Craibia zimmermannii*	29.09	53.33	25.45	63.64	60.00	16.18	62.50	58.82
10	*Ocotea usambaransis*	70.40	84.86	82.06	86.32	36.77	37.27	69.70	71.88
	Overall Accuracy	**79.47**		**80.15**		**49.24**		**80.00**	

4.2.1 Optimization of Random Forest Classification Models

All RF classification models obtained the same optimal *ntree* values for all species in this study across all band combinations. The *ntree* value of 500 while *mtry* values of 1 was achieved for classification using 129 and 53 bands (Figure 4.5). The 500 *ntree* had the least OOB errors compared to the others, therefore it was selected for further analysis.

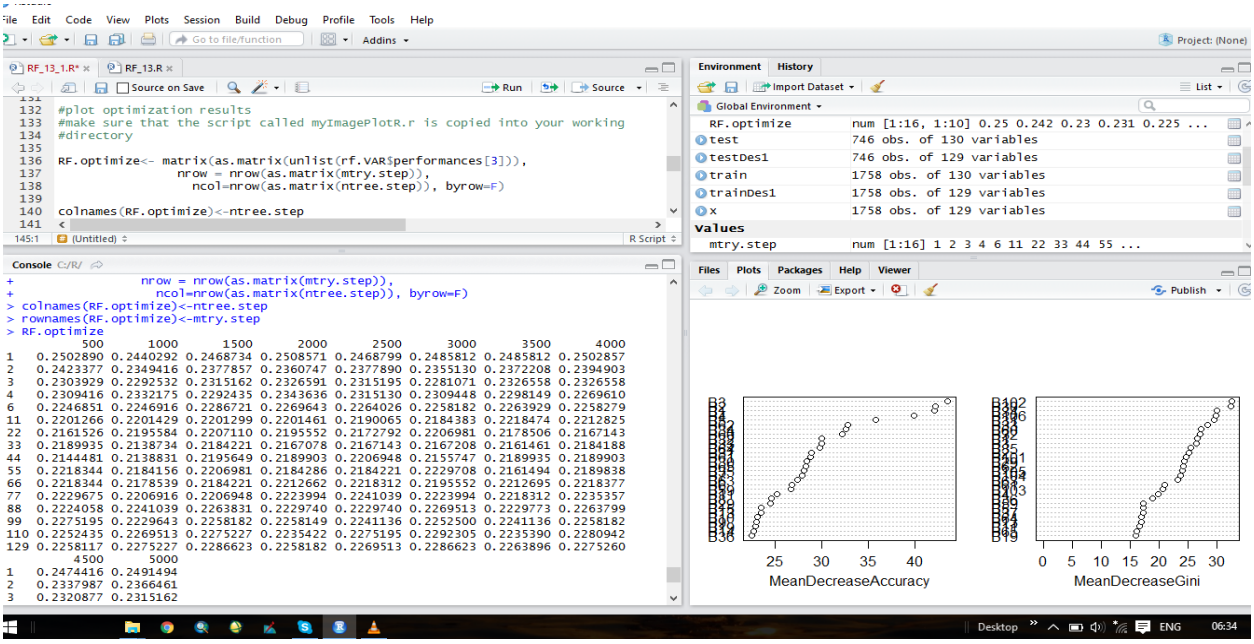

Figure 4.5: ntree values for different model settings used in the selection of suitable bands.

4.2.2 Accuracy Assessment

The overall accuracy of the Ngangao Forest RF classification algorithm was 80.00% (0.77 kappa coefficient) when using the 129 bands and 78.15% (0.74 kappa coefficient) when using 53 bands. The thematic map from the AISA Eagle is presented in Figure 4.6. *Macaranga capensis* and *Ficus thoningii* were the dominant species in Ngangao Forest. *Pinus patula* species was overly present in the classification map, spreading to the croplands and shrublands. Generally *Craibia zimmermannii*, *Macaranga capensis* and *Phoenix reclinata* had the lowest user and producer accuracies while *Albizia gummifera*, *Newtonia buchananii* and *Pinus patula* had the highest accuracies. The specific classification accuracies of species were slightly lower when using 53 bands compared with the 129 bands. *Syzygium guineense*, *Ficus thoningii*, *Macaranga capensis*,

Albizia gummifera and *Craibia zimmermannii* were majorly restricted to the forested area. The confusion matrices of the classification map (Figure 4.6) are presented in Tables 4.2 and 4.3.

Individual accuracies (PA and UA) were generally high (over 60%) for most of the tree species except *Acacia mearnsii* (UA=36.5%), *Craibia zimmermannii* (UA=18%) and *Phoenix reclinata* (UA=55.1%) indicating confusion with other classes.

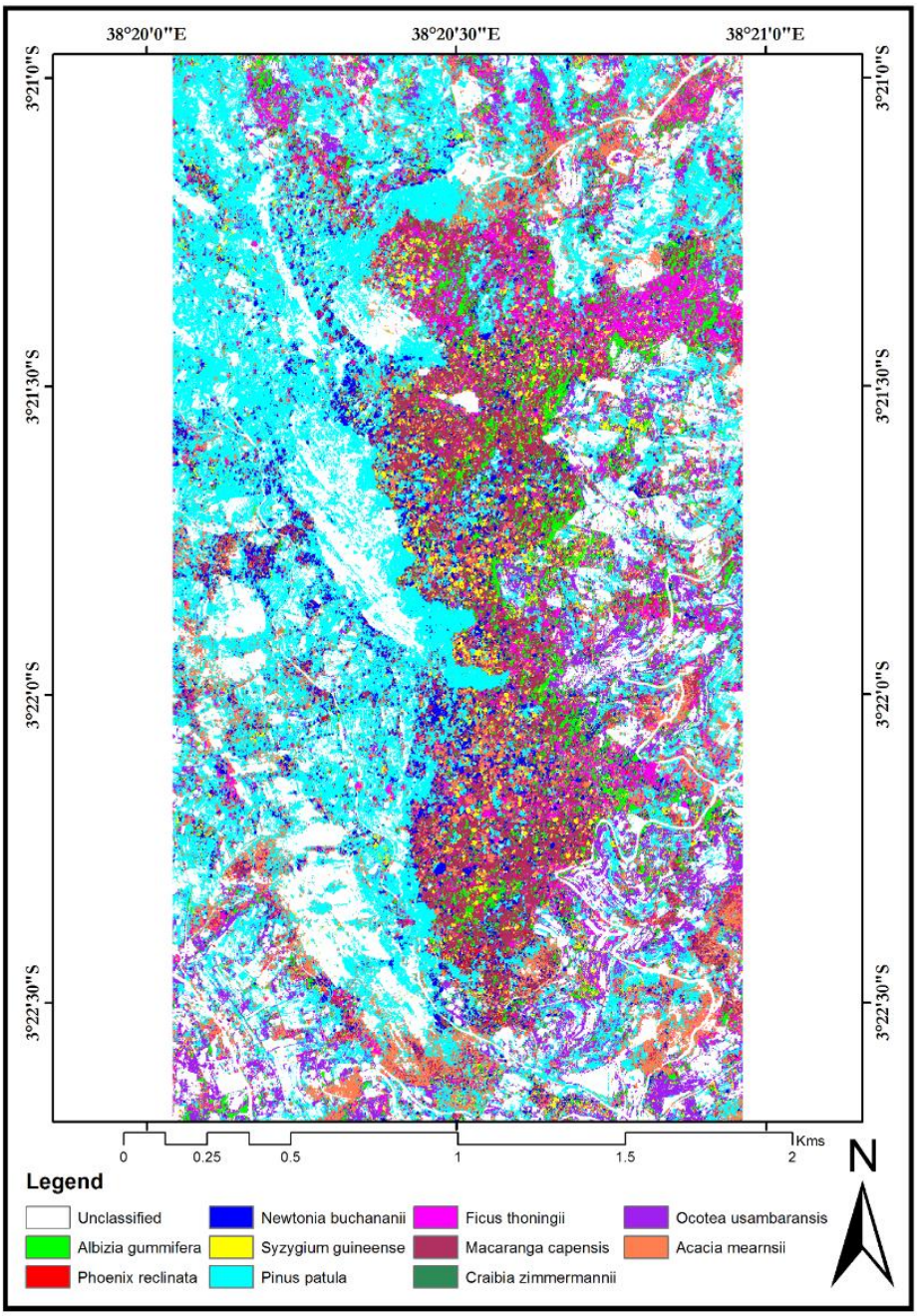

Figure 4.6: Classification map of the Ngangao Forest using random forest classifier

Table 4.2: Individual species producer and user accuracies of the random forest classifier.

			129 Bands		53 Bands	
	Species Name	**Total Points Used**	**Producer Accuracy (%)**	**User Accuracy (%)**	**Producer Accuracy (%)**	**User Accuracy (%)**
1	*Acacia mearnsii*	136	65.00	65.00	60.00	61.54
2	*Albizia gummifera*	269	90.00	85.71	90.00	85.71
3	*Craibia zimmermannii*	55	62.50	58.82	50.00	61.54
4	*Ficus thoningii*	347	86.54	76.27	84.62	72.73
5	*Macaranga capensis*	241	58.33	79.25	55.56	78.43
6	*Newtonia buchananii*	253	86.67	92.86	86.67	90.28
7	*Ocotea usambarensis*	223	69.70	71.88	69.70	73.02
8	*Phoenix reclinata*	69	50.00	58.82	50.00	66.67
9	*Pinus patula*	657	94.92	85.00	94.92	82.02
10	*Syzygium guineense*	254	64.47	77.78	60.53	76.67
Overall accuracy				**80.00**		**78.15**

Table 4.3: Classification confusion matrix of the Random Forest classifier using the AISA Eagle image.

	A	B	C	D	E	F	G	H	I	K	Total	UA(%)
(a)	**Using all (129) AISA Eagle wavebands**											
A	26	0	1	1	9	0	0	0	2	1	**40**	65.00
B	0	72	2	1	8	1	0	0	0	0	**84**	85.71
C	2	1	10	2	0	0	1	0	0	1	**17**	58.82
D	3	0	2	90	8	5	4	1	4	1	**118**	76.27
E	2	4	0	0	42	2	0	1	1	1	**53**	79.25
F	0	3	0	0	0	65	0	2	0	0	**70**	92.86
G	0	0	0	3	1	0	46	0	3	11	**64**	71.88
H	0	0	0	1	3	0	0	10	0	3	**17**	58.82
I	6	0	1	4	0	1	12	0	187	9	**220**	85.00
K	1	0	0	2	1	1	3	6	0	49	**63**	77.78
Total	**40**	**80**	**16**	**104**	**72**	**75**	**66**	**20**	**197**	**76**	**746**	
PA(%)	65.00	90.00	62.50	86.54	58.33	86.67	69.70	50.00	94.92	64.47		
OA(%)	80.00											
(b)	**Using the most important (53) AISA Eagle wavebands**											
A	24	0	0	3	8	0	0	0	3	1	**39**	61.54
B	0	72	1	1	8	2	0	0	0	0	**84**	85.71
C	2	1	8	1	0	0	1	0	0	0	**13**	61.54
D	5	0	4	88	10	4	3	1	2	4	**121**	72.73
E	2	4	0	0	40	2	0	1	0	2	**51**	78.43
F	0	3	1	0	1	65	0	2	0	0	**72**	90.28
G	0	0	0	4	1	0	46	0	5	7	**63**	73.02
H	0	0	0	0	3	0	0	10	0	2	**15**	66.67
I	6	0	1	5	0	1	14	0	187	14	**228**	82.02

K	1	0	1	2	1	1	2	6	0	46	**60**	76.67
Total	**40**	**80**	**16**	**104**	**72**	**75**	**66**	**20**	**197**	**76**	**746**	
PA (%)	60.00	90.00	50.00	84.62	55.56	86.67	69.70	50.00	94.92	60.53		
OA (%)	**78.55**											

Legend:

A	*Acacia mearnsii*	**F**	*Newtonia buchananii*
B	*Albizia gummifera*	**G**	*Ocotea usambarensis*
C	*Craibia zimmermannii*	**H**	*Phoenix reclinata*
D	*Ficus thoningii*	**I**	*Pinus patula*
E	*Macaranga capensis*	**K**	*Syzygium guineense*

4.3 Mapping Tree Species using Simulated Multispectral Data

Resampling the images from hyperspectral to multispectral reduced the image size (disk) from 2.25 gigabytes to 21.40 megabytes for Worldview 2 and 1.40 megabytes for the Sentinel 2 image. The processing speed improved as the load on the computer reduced. Three classification methods {i.e. (a) Spectral Angle Mapper, (b) Neural Network and (c) Support Vector Machine} were used to test the applicability of upscaling of tree species identification in Ngangao Forest from hyperspectral to multispectral images. The hyperspectral image was classified using the three methods and the results are shown in Figure 4.7. Table 4.4 shows the accuracy assessments of the results. The Spectral Angle Mapper classification method output had the lowest accuracy (below 50%). Therefore, this method was eliminated from further analysis. Support Vector Machine proved to have the highest accuracy of 80.15% compared to Neural Network (79.47%). These two methods were used to test the applicability of upscaling species identification in tree species in Ngangao Forest.

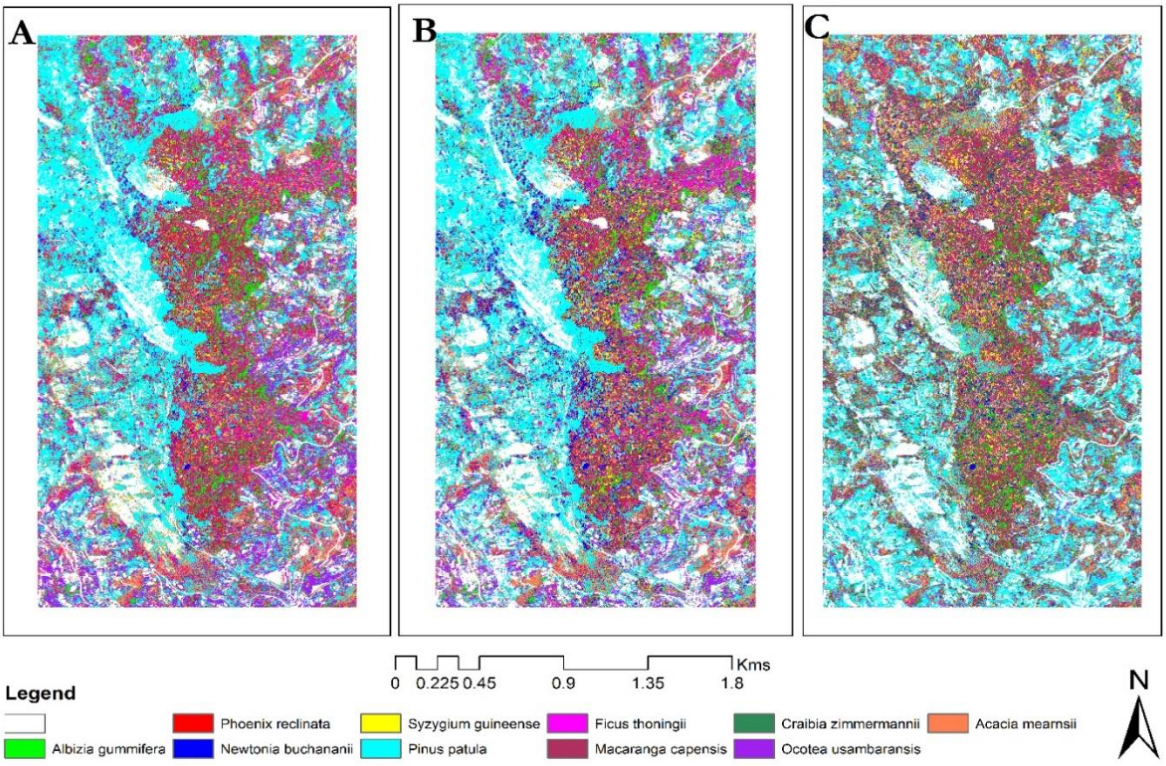

Figure 4.7: Classified images of tree species using AISA Eagle hyperspectral data: A) SAM, B) NN, C) SVM

Table 4.4: Individual class accuracy of tree species classification in Ngangao Forest.

	2013	**A) Spectral Angle Mapper**		**B) Neural Network**		**C) Support Vector Machine**	
	Species Name	Producer Accuracy	User Accuracy	Producer Accuracy	User Accuracy	Producer Accuracy	User Accuracy
1	*Albizia gummifera*	52.42	42.34	95.17	76.42	89.22	78.18
2	*Phoenix reclinata*	26.09	60.00	55.07	45.78	33.33	69.70
3	*Newtonia buchananii*	69.57	67.69	71.94	93.81	79.45	75.00
4	*Syzygium guineense*	39.76	33.44	71.26	69.35	74.80	72.52
5	*Pinus patula*	72.75	84.90	98.02	89.94	97.72	90.17
6	*Ficus thoningii*	27.38	49.48	77.23	72.63	71.76	80.58
7	*Macaranga capensis*	29.46	33.65	62.24	82.87	66.80	74.54
8	*Acacia mearnsii*	27.94	20.11	72.06	65.33	76.47	63.80
9	*Craibia zimmermannii*	60.00	16.18	29.09	53.33	25.45	63.64
10	*Ocotea usambaransis*	36.77	37.27	70.40	84.86	82.06	86.32
	Overall Accuracy		**49.24**		**79.47**		**80.15**
	Kappa Coefficient		**0.42**		**0.76**		**0.77**

Support Vector Machine crushed during the classification of Sentinel 2 image. Therefore, it was eliminated from further analysis. On the other hand, Neural Network successfully classified the Worldview 2 and Sentinel 2 images. Generally, the overall classification accuracy and Kappa coefficient of Worldview 2 was higher than that of Sentinel 2 (Table 4.5). Even though the spatial resolution of Sentinel 2 was lower than Worldview 2 and the training sites were fewer, the interclass accuracies of some species were high in Sentinel 2 than in Worldview 2. On the other hand, some classes had 0% accuracy for both producer and user accuracies in Sentinel 2. Moreover, two classes did not classify in the Sentinel 2 image.

Training sites reduced progressively from the hyperspectral image, Worldview 2 image to the Sentinel 2 image (Table 4.6). *Albizia gummifera* and *Pinus patula* had the highest accuracies in the Worldview 2 classification while *Phoenix reclinata* had the lowest accuracy. *Acacia mearnsii* and *Crabia zimmermannii* had 0% accuracy in this classification. On the other hand, *Newtonia buchananii, Syzygium guineense, Ficus thoningi* and *Acacia mearnsii* had 0% accuracy in the Sentinel 2 classification while *Phoenix reclinata* and *Crabia zimmermannii* did not classify

because the scaling of the images from AISA Eagle to Sentinel 2 increased the pixel size of the image beyond the training sites the diameter ranges of the training sites.

Worldview 2 classification map (Figure 4.8 A) shows that features were distinguishable and classes separable at that level. On the other hand, the Sentinel 2 classification map did not distinguish between features clearly, while some of the classes were not clearly separable (Figure 4.8 B). This was mainly because the difference between cell resolution canopy sizes of some of the tree species was small.

Table 4.5: Classification accuracies of tree species in Ngangao forest using Worldview 2 and Sentinel 2.

	2013	**Worldview 2**		**Sentinel 2**	
	Species Name	Producer Accuracy	User Accuracy	Producer Accuracy	User Accuracy
1	*Albizia gummifera*	95.77	66.67	75.00	75.00
2	*Phoenix reclinata*	5.88	100.00	Did not classify	Did not classify
3	*Newtonia buchananii*	23.81	83.33	0.00	0.00
4	*Syzygium guineense*	59.32	33.02	0.00	0.00
5	*Pinus patula*	94.77	85.34	100.00	71.43
6	*Ficus thoningii*	54.12	29.30	100.00	36.00
7	*Macaranga capensis*	30.88	45.65	0.00	0.00
8	*Acacia mearnsii*	0.00	0.00	0.00	0.00
9	*Craibia zimmermannii*	0.00	0.00	Did not classify	Did not classify
10	*Ocotea usambaransis*	19.30	78.57	0.00	0.00
	Overall Accuracy		**56.43**		**47.22**
	Kappa Coefficient		**0.48**		**0.33**

Table 4.6: Training sites used to classify tree species in Ngangao Forest.

	Species Name	RoIs AISA Eagle	RoIs Worldview 2	RoIs Sentinel 2
1	*Albizia gummifera*	269	71	4
2	*Phoenix reclinata*	69	17	0
3	*Newtonia buchananii*	253	63	4
4	*Syzygium guineense*	254	59	2
5	*Pinus patula*	657	172	4
6	*Ficus thoningii*	347	85	5
7	*Macaranga capensis*	241	68	1
8	*Acacia mearnsii*	136	15	1
9	*Craibia zimmermannii*	55	57	0
10	*Ocotea usambaransis*	223	31	2

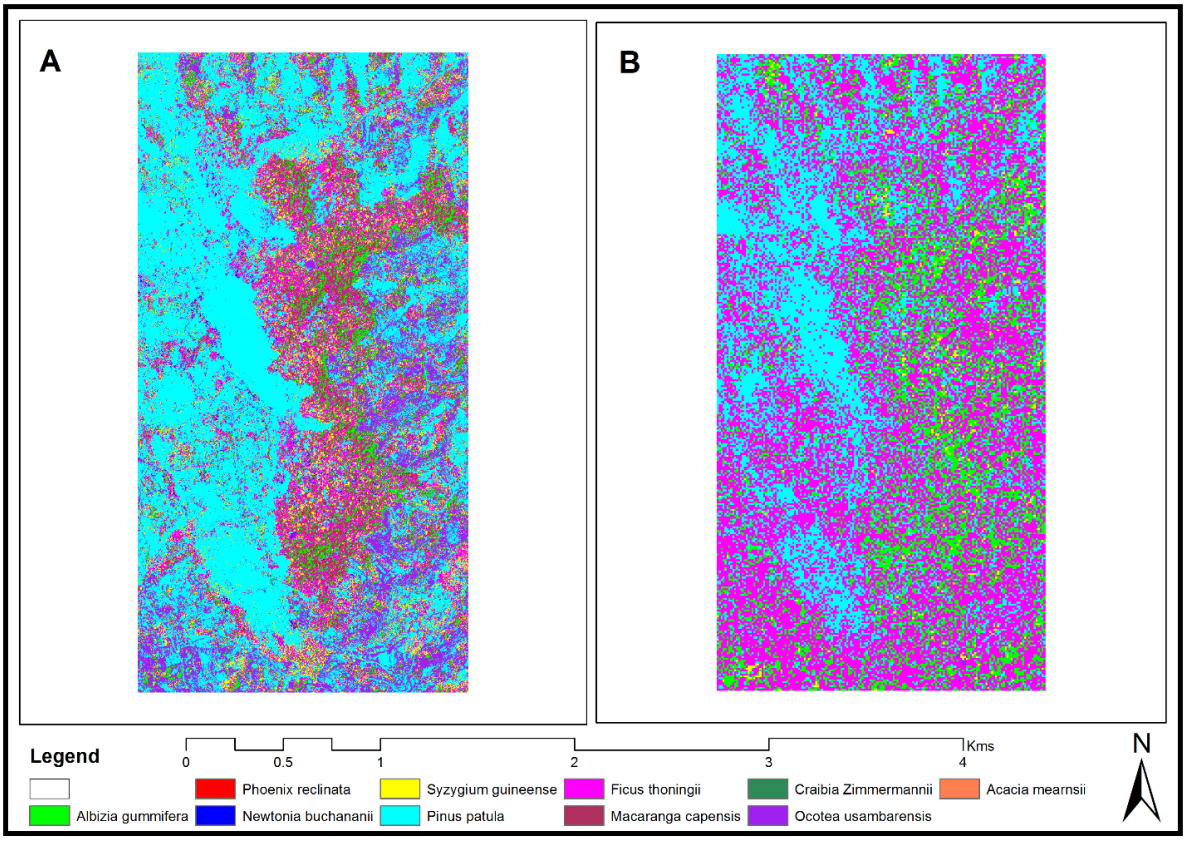

Figure 4.8: Thematic maps for the classification of tree species using different multispectral images: A) Worldview 2, B) Sentinel 2.

CHAPTER FIVE

DISCUSSIONS OF THE RESULTS

5.1 Selection of Sensitive Spectral Bands for Tree Species Mapping in Ngangao Forest

The decreasing dimensionality of the hyperspectral AISA Eagle image (n=53 bands) had results with similar accuracies as the original image with all the spectral bands (n=129 bands). This meant that the data dimensionality was reduced by 41.1%, a dimension similar to that (Abdel-Rahman et al., 2015) found when using data from the same sensor with 64 bands (n=64), to map flowering plants in the Kenyan savannah. Dimensionality reduction ensures that grid search and cross validation computation costs of the RF classification algorithm optimization are reduced, even though some of the selected bands were found to be correlated and therefore contain the same information as shown in Figure 4.4.

5.2 Mapping Selected Tree Species in Ngangao Forest

The relatively high OA's and individual class accuracies (UA and PA) alluded to the fact that AISA Eagle image and the RF classifier has the potential to map tree species in forested areas. This study, demonstrated the heftiness of the .632+ bootstrap method in reducing the data dimensionality in hyperspectral data in the RF classifier, in line with the (Abdel-Rahman et al., 2015) research. Even though it is expected that tree species discrimination could have been significantly improved with the inclusion of the SWIR regions of the EMS, the image acquisition cost could have substantially increased. This is because image acquisition could have required the flying altitude to be three times lower to achieve the desired spatial resolution as per the specification of the SWIR sensor. The IR region of the AISA Eagle EMS proved to be vital in substantiating this lacuna as could be seen in Figure 4.2 of the waveband usefulness and selection (Ge et al., 2006). The visible, red edge and IR regions of the EMS are sensitive to chlorophyll and other leaf properties (Filella and Penuelas, 1994; Kumar et al., 2002).

Even though the overall accuracies were relatively high, the individual accuracies (PA and UA) of some tree species such as (*Craibia zimmermannii* and *Phoenix reclinata*) were low. This could be attributed to the confusion of such classes with other tree species or other plants such as crops. In particular the classification map (Figure 4.6) above showed that *Phoenix reclinata* was over-mapped into farmlands and other landcover classes that the tree was not observed. This could also

be due to the auto-correlation between selected bands that were important in the classification, especially from the green and red regions of the EMS. Additionally the canopy structure of different tree species could have affected the mapping ability of some of the species, whose spectral responses (Kumar et al., 2002; Petropoulos et al., 2014) were affected by their canopy geometry. Moreover, the application of pixel based classification could result in misclassification (Cho et al., 2012) as the pixels at the border of the canopies have high intra-class variability. This could also lead to the salt and pepper effect (de Jong et al., 2011; Ouyang et al., 2011; Piiroinen et al., 2015) in regions without well-defined pixel orientation when defining the classes.

In this study, a combination of high spectral (n=129) and spatial resolutions (1m), coupled with optimized machine learning algorithm approach was used. The robustness in this blend ensured that tree species were separable at fine scales. In cognisant that the SWIR part of the EMS could have produced better results, it is suggested that future studies include the SWIR bands to discriminate tree species. However, this approach is expensive and time consuming since AISA Eagle hyperspectral image is not readily available and optimizing the robust RF algorithm is costly. Therefore, upscaling this method to the multispectral images such as Worldview 3 and Sentinel 2 that are accessible or freely available should be investigated.

The RF algorithm in this study was developed to map different tree species in Ngangao Forest. This information is required to understand the distribution of different tree species in the landscape matrix and their health to develop a conservation framework for different tree species and landscape integrity. Tree species spatial-temporal information is valuable for conservation and ecological assessments which will ultimately lead to sustainable landscapes and controlled resource utilization at various landscapes and biodiversity establishment.

5.3 Mapping of Tree Species using Simulated Multispectral Data

5.3.1 Disk size and processing speed

Resampling, transforms the image dimension on various axes. For instance, upscaling introduces more pixels to the image while downscaling leads to pixel reduction (Wu and Li, 2009). Resampling the Ngangao Forest hyperspectral data to multispectral data involved both spectral and spatial dimensional reduction. The image was downscaled both spatially and spectrally leading

to a reduction in image size (Veganzones et al., 2016; Zhang et al., 2017). The number of bands in the simulated data was smaller than the bands in the hyperspectral data. Most of the bands in the hyperspectral data were redundant, hence when they are resampled the information therein was consolidated into fewer bands. This meant that the smaller simulated images were processed by the classification algorithm with ease compared to the larger hyperspectral images.

5.3.2 Dimensionality

Dimensionality reduction minimizes the problems of nonlinearity, redundancy of bands and high dimensions in hyperspectral data (Wang and Wang, 2015; Yanqin and Ping, 2005), which in turn leads to data sets that are smaller in size compared to the original files, without loss of important information (Benedetto and Czaja, 2013). Resampling the Ngangao forest image reduced it spectrally from 129 bands to 8 bands for Worldview 2. The classified image of the resampled data achieved more than 56% accuracy in species identification compared to the 78% accuracy achieved by the hyperspectral data. This is despite the reduction in spatial resolution of the resampled image which might have contributed to the reduction in accuracy. (Mumby and Edwards, 2002) showed that spatial resolution improves the amount of details an image contains, while (McCloy and Bøcher, 2007) demonstrated how this resolution improves within class accuracy. More details improve the algorithms ability to discriminate between classes because the signatures of the different classes are better defined. Contrary, a reduction of the image details that discriminate between species classes will lead to a low ability of the algorithm to identify and differentiate between classes, hence lower accuracy.

5.3.3 Classification methods and machine learning algorithms

As a machine learning algorithm, Support Vector Machine (Colgan et al., 2012; Denghui and Le, 2011) utilizes signature data provided in the training sample to build separable units that are used in the classification. On the other hand, Artificial Neural Network (Abraham, 2005; Yegnanarayana, 2009) simulates animal brains to progressively build information from signatures provided for by the training samples. Even though Support Vector Machine achieved the highest accuracy when the Worldview 2 image of Ngangao Forest was classified, the algorithm was not able to classify the simulated sentinel 2 image which had more spectral bands than Worldview 2 but less spatial resolution. On the other hand, Neural Network which was ranked second in this

classification, managed to classify the image well with a small reduction in accuracy. Artificial Neural Network is reputed to optimize training sites to obtain high accuracy without the need for too much information (Nguyen et al., 2006). Therefore, Artificial Neural Network optimized the training sites to classify the Sentinel 2 image better than Support Vector Machine.

5.3.4 Training sites

Supervised classification is guided by specific spectral signatures which are representatives of the desired or available landcover classes in an image (Chi and Bruzzone, 2007; Mantero et al., 2005). These representative classes, which are also called training sites, guide the algorithm in the identification of similar pixels throughout the image, which are grouped into one class. In the Ngangao Forest image, the training sites were collected using the hyperspectral image whose spatial resolution was 1 metre. These sites were collected based on the pixel properties of the image, and considering that the canopy sizes of most of the trees was less than 10 metres, therefore most sites were less than the canopy sizes of these trees. In fact, to obtain pure pixels, only a subset of the canopy was considered as training sites.

To classify the resampled Worldview 2 image, whose resolution was less than 2 metres, and Sentinel 2 whose resolution was 10 metres, the training sites were scaled to these images using the scaling application. Therefore, those training sites whose size was smaller than the resolution of the respective scaled images were automatically eliminated. This resulted into a total of 638 in Worldview 2 and 23 in Sentinel 2, down from 2,504 training sites in AISA Eagle image.
Some of the classes did not have any training sites to classify the Sentinel 2 image such as *Phoenix reclinata,* and *Craibia zimmermannii,* while some, such as *Macaranga capensis* and *Acacia mearnsii* had very few training sites. This affected the overall accuracy of the classification since the training sites that were used in the classification were also used in verification. This led to some of the tree species classes being classified with higher accuracy in Sentinel 2 than in Worldview 2.

Increasing the training sites of these images to achieve better representation was not possible since the pixel sizes were bigger than the canopies of some of the trees used to pick pure pixel. However, some of the classes which had bigger sized tree canopies as training sites (such as *Albizia*

gummifera) gave impressive accuracies. Therefore, it is possible to upscale the tree species identification to Sentinel 2 using big sized tree canopies as training sites.

5.3.5 Map description

The maps in Figure 4.8 show that species identification and segregation in Ngangao forest was successfully done using multispectral images. On one hand, the shape of the forest was distinct in Worldview 2 than in Sentinel 2. On the other hand, *Ficus thoningii* and *Albizia gummifera* species was over-classified in Sentinel 2 as compared to other species. This was attributable to the close similarity between the spectral reflectance of these species with farmlands around the forest. Since the training sites were reduced in Sentinel 2 compared to Worldview 2, distinguishing between tree species classes in the forest and crops in the farmlands was not clear. Therefore, they were classed as similar classes. This could however have been improved had the spatial resolution of the Sentinel 2 images been high. It is suspected that resampling the Sentinel 2 images with higher spatial resolution (probably between 2 to 5 metres) would improve the classification accuracy of tree species.

CHAPTER SIX
CONCLUSIONS AND RECOMMENDATIONS

6.1 Conclusions

The impacts of climate change in the African continent have far reaching effects because it is a region of high vulnerability to climate shocks; it threatens food security, livelihoods and economic prosperity. African forest ecosystems, which are interlinked to food production systems, are among the most impacted by world climate change. More so, the indigenous tree species are at a high risk of extinction hence the need to quantify them for conservation purposes. Modern methods such as remote sensing and specifically hyperspectral remote sensing offers a more accurate method with expansive scope for conservation, compared to the tedious and time-consuming methods that were previously used. Generally, this study aimed at mapping the indigenous and exotic tree species appearing on the top canopy of the Ngangao Forest using airborne hyperspectral data. Specifically, it aimed at determining the most appropriate spectral bands from the hyperspectral data for mapping of selected tree species; mapping selected tree species using different classification algorithms and selected appropriate spectral bands; and finally testing the potential application of simulated multispectral data to discriminate tree species in Ngangao Forest.

Ngangao Forest is located in Taita Hills in the coastal region and approximately 100 kilometres from Kilimanjaro Mountain. It receives bimodal rainfall with *Acacia mearnsii* and *Pinus patula* being the main tree species in the area. For this study, the following tree species were considered; *Acacia mearnsii, Cupressus lusitanica, Eucalyptus spp, Pinus patula, Albizia gummifera, Ficus thonningi, Macaranga capensis, Newtonia buchananii, Ocotea usambarensis and Syzygium guineense.* Hyperspectral images were acquired using Airborne Imaging Spectrometer for Applications (AISA) Eagle VNIR sensor on 4th February 2013 at a mean flying height of approximately 2300 m above sea level. High definition photographs that were taken in January 2012, were used in combination with insitu data and expert knowledge to delineate and pick training sites. The images were subjected to radiometric and atmospheric correction using CaliGeo Pro and ATCOR-4 software respectively. Orthorectification was consequently performed using a 20m DEM resampled to 1m spatial resolution. Worldview 2 and Sentinel 2 multispectral images were resampled from the hyperspectral AISA Eagle image and used to test the upscaling of the mapping algorithms. Neural Network, Support Vector Machine, Spectral Angle Mapper and Random Forest algorithms were used for the same test.

Results indicated that mapping of tree species in Ngangao Forest was successful using images of different spatial and spectral resolution. The Spectral Angle Mapper algorithm achieved the lowest accuracy in mapping of the tree species while Random Forest and Support Vector Machine achieved the highest accuracies. The hyperspectral images achieved the highest accuracies using the Random Forest algorithm while the multispectral images achieved low accuracies. Sentinel 2 image achieved the lowest accuracy because of the low spatial resolution and fewer number of training sites with low purity of the end members of each species. The Random Forest algorithm produced desirable results with the reduction of bands to 53 and good spectral separability. *Macaranga capensis* and *Ficus thoningii* were the most dorminant species in Ngangao Forest. The highest class accuracies were recorded for *Pinus patula* and *Newtonia buchananii* while those for *Crabia zimmermanni* and *Phoenix reclinata* were the lowest. In the multispectral images, World View 2 achieved better classification accuracy compared to Sentinel 2.

This research has demonstrated the possibility of using hyperspectral data to map trees species in Kenyan tropical forest. As stated earlier in this research, there is no documented evidence of using this technology to map trees in East Africa. Different algorithms have also been tested in this research and the outcome could inform other researchers on the preferable algorithm of the four tested algorithms. Finally, this research has also compared two multispectral sensors and shows that one would give preference to World View 2 images as they exhibit better results.

6.2 Recommendations

Hyperspectral image classification achieved the highest class accuracies compared to multispectral images. Moreover, hyperspectral image with all the 129 bands had better class accuracy compared to the 53 band image classification. Even though the hyperspectral images achieved the highest accuracy when using the highest possible number of spectral bands, they are highly unavailable because of the cost of acquiring them and dimensional redundancies. The collinearity effect exhibited by hyperspectral images with many bands pose a very big challenge. Therefore, an algorithm that enables the selection of the most appropriate bands based on the specific species class information is paramount to increasing the accuracy of species identification.

Even though more class specific training data means an increase in collinearity, better methods should be devised to ensure more class information, that is explicitly accurate is collected to reduce

the divergence of class reflectance from the mean. Additionally, to achieve higher accuracy in species identification, studies should be focused on specific classes, while classification should be done on individual classes as opposed to combining all class information together. Novel methods such as spectrometry and Analytical Spectral Devices (ASD) should be used to increase the purity of end members. It is also recommended that a combination of Light Detection and Ranging (LiDAR) and hyperspectral data could be tested to find out whether the result would improve. It is also recommended that object-based classification approaches be used to map the tree species using hyperspectral data in order to compare the results of the pixel based approaches used in this research.

This research could be extended to other forest fragments in Taita Hills and other tropical forest ecosystems. The findings of this research could be useful to other researchers who are keen on evaluating ecosystem services offered by forests. In addition, the institutions tasked with the management and conservation of forest ecosystems such as Kenya Forest Service, National Museums of Kenya and Kenya Wildlife Service could also benefit from the results of the research in their performance of their core mandates.

6.3 Research Contribution to Knowledge

The three objectives of this research were achieved. Generally, the results of this study have contributed to the body of knowledge in the following ways. First, this study has demonstrated the possibility of mapping trees species in tropical forest ecosystems using airborne hyperspectral data. By the time of submitting this thesis, there was no documented evidence of the technology being used in East Africa to map the species. Secondly, different methods were tested to reduce the high dimensionality of hyperspectral data. Additionally, different algorithms were used together with selected bands to map the individual tree species. The only documented research in this field and geographic region was by Abdel-Rahman et al. (2015) who tested the Random Forest algorithm only and airborne hyperspectral data (processed to 64 bands) in flower mapping in Lower Eastern Kenya. This research has showed that Random Forest algorithm performed well in the selection of sensitive bands and also in the mapping of tree species appearing on the top canopy of Ngangao Forest. These results could advise other researchers on the preferable algorithm (of the tested ones) to use in a similar ecosystem. Thirdly, the research has also shown that the more affordable sensors

such as WorldView 2 can be used to map tree species but with relatively low accuracies. Sentinel 2 sensor performed poorly in mapping of tree species in the tropics.

REFERENCES

Abdel-Rahman, E.M., Makori, D.M., Landmann, T., Piiroinen, R., Gasim, S., Pellikka, P., Raina, S.K., 2015. The Utility of AISA Eagle Hyperspectral Data and Random Forest Classifier for Flower Mapping. Remote Sensing 7, 13298–13318. https://doi.org/10.3390/rs71013298

Abraham, A., 2005. Artificial neural networks. handbook of measuring system design.

Al, W., ORKING, G., CLIMA, O., 2008. Climate change and food security: a framework document. FAO Rome.

Amarsaikhan, D., Douglas, T., 2004. Data fusion and multisource image classification. International Journal of Remote Sensing 25, 3529–3539.

Asner, G.P., Martin, R.E., 2012. Contrasting leaf chemical traits in tropical lianas and trees: implications for future forest composition. Ecology Letters 15, 1001–1007.

Atkinson, P.M., Tatnall, A.R.L., 1997. Introduction Neural networks in remote sensing. International Journal of Remote Sensing 18, 699–709. https://doi.org/10.1080/014311697218700

Bannari, A., Morin, D., Bonn, F., Huete, A. R., 1995. A review of vegetation indices. Remote Sensing Reviews, 13(1), 95–120.

Bartholomé, E., Belward, A.S., 2005. GLC2000: a new approach to global land cover mapping from Earth observation data. International Journal of Remote Sensing 26, 1959–1977.

Becker, B.L., Lusch, D.P., Qi, J., 2007. A classification-based assessment of the optimal spectral and spatial resolutions for Great Lakes coastal wetland imagery. Remote Sensing of Environment 108, 111–120. https://doi.org/10.1016/j.rse.2006.11.005

Behnia, P., 2005. Comparison between four methods for data fusion of ETM+ multispectral and pan images. Geo-Spatial Information Science 8, 98–103.

Benedetto, J.J., Czaja, W., 2013. Dimension Reduction and Remote Sensing Using Modern Harmonic Analysis, in: Freeden, W., Nashed, M.Z., Sonar, T. (Eds.), Handbook of Geomathematics. Springer Berlin Heidelberg, pp. 1–22. https://doi.org/10.1007/978-3-642-27793-1_50-1

Benediktsson, J.A., Sveinsson, J.R., Ersoy, O.K., Swain, P.H., 1997. Parallel consensual neural networks. IEEE Transactions on Neural Networks 8, 54–64.

Beniwal, S., Arora, J., 2012. Classification and feature selection techniques in data mining. International journal of engineering research & technology (ijert) 1.

Boardman, J.W., 1994. Geometric mixture analysis of imaging spectrometry data, in: Geoscience and Remote Sensing Symposium, 1994. IGARSS'94. Surface and Atmospheric Remote Sensing: Technologies, Data Analysis and Interpretation., International. IEEE, pp. 2369–2371.

Breiman, L., 2001. Random Forests. Machine Learning 45, 5–32. https://doi.org/10.1023/A:1010933404324

Burgess, P.W., Dumontheil, I., Gilbert, S.J., 2007. The gateway hypothesis of rostral prefrontal cortex (area 10) function. Trends in cognitive sciences 11, 290–298.

Camps-Valls, G., Bruzzone, L., 2005. Kernel-based methods for hyperspectral image classification. IEEE Transactions on Geoscience and Remote Sensing 43, 1351–1362.

Camps-Valls, G., Gomez-Chova, L., Muñoz-Marí, J., Vila-Francés, J., Calpe-Maravilla, J., 2006. Composite kernels for hyperspectral image classification. IEEE Geoscience and Remote Sensing Letters 3, 93–97.

Černá, L., Chytrý, M., 2005. Supervised classification of plant communities with artificial neural networks. Journal of Vegetation Science 16, 407–414.

Chang, C.-I., 2003. Hyperspectral Imaging: Techniques for Spectral Detection and Classification. Springer Science & Business Media.

Chang, C.-I., Plaza, A., 2006. A fast iterative algorithm for implementation of pixel purity index. IEEE Geoscience and Remote Sensing Letters 3, 63–67.

Chen, C.M., Kovacevic, R., 2003. Finite element modeling of friction stir welding—thermal and thermomechanical analysis. International Journal of Machine Tools and Manufacture 43, 1319–1326.

Chi, M., Bruzzone, L., 2007. Semisupervised classification of hyperspectral images by SVMs optimized in the primal. IEEE Transactions on Geoscience and Remote Sensing 45, 1870–1880.

Cho, M.A., Mathieu, R., Asner, G.P., Naidoo, L., van Aardt, J., Ramoelo, A., Debba, P., Wessels, K., Main, R., Smit, I.P.J., Erasmus, B., 2012. Mapping tree species composition in South African savannas using an integrated airborne spectral and LiDAR system. Remote Sensing of Environment 125, 214–226. https://doi.org/10.1016/j.rse.2012.07.010

Chu, C., Hsu, A.-L., Chou, K.-H., Bandettini, P., Lin, C., Initiative, A.D.N., 2012. Does feature selection improve classification accuracy? Impact of sample size and feature selection on classification using anatomical magnetic resonance images. Neuroimage 60, 59–70.

Cihlar, J., Guindon, B., Beaubien, J., Latifovic, R., Peddle, D., Wulder, M., Fernandes, R., Kerr, J., 2003. From need to product: a methodology for completing a land cover map of Canada with Landsat data. Canadian Journal of Remote Sensing 29, 171–186.

Cingolani, A.M., Renison, D., Zak, M.R., Cabido, M.R., 2004. Mapping vegetation in a heterogeneous mountain rangeland using Landsat data: an alternative method to define and classify land-cover units. Remote sensing of environment 92, 84–97.

Clark, M.L., Aide, T.M., Grau, H.R., Riner, G., 2010. A scalable approach to mapping annual land cover at 250 m using MODIS time series data: A case study in the Dry Chaco ecoregion of South America. Remote Sensing of Environment 114, 2816–2832. https://doi.org/10.1016/j.rse.2010.07.001

Clark, M.L., Roberts, D.A., Clark, D.B., 2005. Hyperspectral discrimination of tropical rain forest tree species at leaf to crown scales. Remote sensing of environment 96, 375–398.

Clasen, A., Somers, B., Pipkins, K., Tits, L., Segl, K., Brell, M., Kleinschmit, B., Spengler, D., Lausch, A., Förster, M., 2015. Spectral Unmixing of Forest Crown Components at Close Range, Airborne and Simulated Sentinel-2 and EnMAP Spectral Imaging Scale. Remote Sensing 7, 15361–15387. https://doi.org/10.3390/rs71115361

Cohen, J., 1960. A coefficient of agreement for nominal scales. Educational and Psychosocial Measurement, 20, 37-46.

Colgan, M.S., Baldeck, C.A., Féret, J.-B., Asner, G.P., 2012. Mapping savanna tree species at ecosystem scales using support vector machine classification and BRDF correction on airborne hyperspectral and LiDAR data. Remote Sensing 4, 3462–3480.

Congalton, R.G., 1994. Accuracy assessment of remotely sensed data: future needs and directions, in: Proceedings of Pecora. pp. 383–388.

Congalton, R.G., Green, K., 2008. Assessing the Accuracy of Remotely Sensed Data: Principles and Practices, Second Edition. CRC Press.

Dalponte, M., Bruzzone, L., Gianelle, D., 2012. Tree species classification in the Southern Alps based on the fusion of very high geometrical resolution multispectral/hyperspectral images and LiDAR data. Remote sensing of environment 123, 258–270.

Dayhoff, J.E., DeLeo, J.M., 2001. Artificial neural networks. Cancer 91, 1615–1635.

de Jong, R., de Bruin, S., de Wit, A., Schaepman, M.E., Dent, D.L., 2011. Analysis of monotonic greening and browning trends from global NDVI time-series. Remote Sensing of Environment 115, 692–702. https://doi.org/10.1016/j.rse.2010.10.011

DeFries, R., Hansen, M., Townshend, J., 1995. Global discrimination of land cover types from metrics derived from AVHRR pathfinder data. Remote Sensing of Environment 54, 209–222.

DeFries, R.S., Townshend, J.R.G., Hansen, M.C., 1999. Continuous fields of vegetation characteristics at the global scale at 1-km resolution. Journal of Geophysical Research: Atmospheres 104, 16911–16923.

Deng, H., Runger, G., 2012. Feature selection via regularized trees, in: The 2012 International Joint Conference on Neural Networks (IJCNN). Presented at the The 2012 International Joint Conference on Neural Networks (IJCNN), pp. 1–8. https://doi.org/10.1109/IJCNN.2012.6252640

Denghui, Z., Le, Y., 2011. Support vector machine based classification for hyperspectral remote sensing images after minimum noise fraction rotation transformation, in: Internet Computing & Information Services (ICICIS), 2011 International Conference On. IEEE, pp. 132–135.

Diaz-Uriarte, R., Diaz-Uriarte, M.R., 2010. Package 'varSelRF.' Citeseer.

Dye, M., Mutanga, O., Ismail, R., 2011. Examining the utility of random forest and AISA Eagle hyperspectral image data to predict Pinus patula age in KwaZulu-Natal, South Africa. Geocarto International 26, 275–289. https://doi.org/10.1080/10106049.2011.562308

Efron, B., Tibshirani, R., 1997. Improvements on Cross-Validation: The 632+ Bootstrap Method. Journal of the American Statistical Association 92, 548–560. https://doi.org/10.1080/01621459.1997.10474007

Egbert, G.D., Erofeeva, S.Y., 2002. Efficient inverse modeling of barotropic ocean tides. Journal of Atmospheric and Oceanic Technology 19, 183–204.

Elith, J., Graham, C.H., Anderson, R.P., Dudík, M., Ferrier, S., Guisan, A., Hijmans, R.J., Huettmann, F., Leathwick, J.R., Lehmann, A., 2006. Novel methods improve prediction of species' distributions from occurrence data. Ecography 129–151.

Fassnacht, F.E., Latifi, H., Stereńczak, K., Modzelewska, A., Lefsky, M., Waser, L.T., Straub, C., Ghosh, A., 2016. Review of studies on tree species classification from remotely sensed data Remote Sensing of Environment 186, 64–87.

Fauvel, M., 2007. Spectral and spatial methods for the classification of urban remote sensing data. Institut National Polytechnique de Grenoble-INPG; Université d'Islande.

Fauvel, M., Chanussot, J., Benediktsson, J.A., 2008. Adaptive pixel neighborhood definition for the classification of hyperspectral images with support vector machines and composite kernel, in: Image Processing, 2008. ICIP 2008. 15th IEEE International Conference On. IEEE, pp. 1884–1887.

Fauvel, M., Chanussot, J., Benediktsson, J.A., 2006. Evaluation of kernels for multiclass classification of hyperspectral remote sensing data, in: Acoustics, Speech and Signal Processing, 2006. ICASSP 2006 Proceedings. 2006 IEEE International Conference On. IEEE, pp. II–II.

Ferwerda, G., Girardin, S.E., Kullberg, B.-J., Le Bourhis, L., De Jong, D.J., Langenberg, D.M., Van Crevel, R., Adema, G.J., Ottenhoff, T.H., Van der Meer, J.W., 2005. NOD2 and toll-like receptors are nonredundant recognition systems of Mycobacterium tuberculosis. PLoS Pathog 1, e34.

Filella, I., Penuelas, J., 1994. The red edge position and shape as indicators of plant chlorophyll content, biomass and hydric status. International Journal of Remote Sensing 15, 1459–1470. https://doi.org/10.1080/01431169408954177

Filippi, A.M., Jensen, J.R., 2006. Fuzzy learning vector quantization for hyperspectral coastal vegetation classification. Remote Sensing of Environment 100, 512–530.

Foody, G.M., 2002. Status of land cover classification accuracy assessment. Remote sensing of environment 80, 185–201.

Gad, S., Kusky, T., 2006. Lithological mapping in the Eastern Desert of Egypt, the Barramiya area, using Landsat thematic mapper (TM). Journal of African Earth Sciences 44, 196–202.

Galvao, R.K.H., Araujo, M.C.U., Jose, G.E., Pontes, M.J.C., Silva, E.C., Saldanha, T.C.B., 2005. A method for calibration and validation subset partitioning. Talanta 67, 736–740.

Ge, S., Everitt, J., Carruthers, R., Gong, P., Anderson, G., 2006. Hyperspectral Characteristics of Canopy Components and Structure for Phenological Assessment of an Invasive Weed. Environ Monit Assess 120, 109–126. https://doi.org/10.1007/s10661-005-9052-1

Geerken, R., Zaitchik, B., Evans, J.P., 2005. Classifying rangeland vegetation type and coverage from NDVI time series using Fourier Filtered Cycle Similarity. International Journal of Remote Sensing 26, 5535–5554.

Girouard, G., Bannari, A., El Harti, A., Desrochers, A., 2004. Validated spectral angle mapper algorithm for geological mapping: comparative study between QuickBird and Landsat-TM, in: XXth ISPRS Congress, Geo-Imagery Bridging Continents, Istanbul, Turkey. pp. 12–23.

Godfray, H.C.J., Beddington, J.R., Crute, I.R., Haddad, L., Lawrence, D., Muir, J.F., Pretty, J., Robinson, S., Thomas, S.M., Toulmin, C., 2010. Food security: the challenge of feeding 9 billion people. science 327, 812–818.

Goel, P.K., Prasher, S.O., Patel, R.M., Landry, J.-A., Bonnell, R.B., Viau, A.A., 2003. Classification of hyperspectral data by decision trees and artificial neural networks to identify weed stress and nitrogen status of corn. Computers and Electronics in Agriculture 39, 67–93.

Gordon, L.J., Steffen, W., Jönsson, B.F., Folke, C., Falkenmark, M., Johannessen, Å., 2005. Human modification of global water vapor flows from the land surface. Proceedings of the National Academy of Sciences of the United States of America 102, 7612–7617.

Gualtieri, J.A., Cromp, R.F., 1999. Support vector machines for hyperspectral remote sensing classification, in: The 27th AIPR Workshop: Advances in Computer-Assisted Recognition. International Society for Optics and Photonics, pp. 221–232.

Hallegatte, S., 2009. Strategies to adapt to an uncertain climate change. Global environmental change 19, 240–247.

Hatfield, J.L., Prueger, J. H., 2010. Value of using different vegetative indices to quantify agricultural crop characteristics at different growth stages under varying management practices, Remote Sensing, 2(2), 562–578.

Hedley, J., Roelfsema, C., Koetz, B., Phinn, S., 2012. Capability of the Sentinel 2 mission for tropical coral reef mapping and coral bleaching detection. Remote Sensing of Environment 120, 145–155.

Hernández-Espinosa, C., Fernández-Redondo, M., Torres-Sospedra, J., 2004. Some experiments with ensembles of neural networks for classification of hyperspectral images. Advances in Neural Networks–ISNN 2004 912–917.

Hughes, G., 1968. On the mean accuracy of statistical pattern recognizers. IEEE Transactions on Information Theory 14, 55–63. https://doi.org/10.1109/TIT.1968.1054102

Immitzer, M., Atzberger, C., Koukal, T., 2012. Tree species classification with random forest using very high spatial resolution 8-band WorldView-2 satellite data. Remote Sensing 4, 2661–2693.

Immitzer, M., Vuolo, F., Atzberger, C., 2016. First Experience with Sentinel-2 Data for Crop and Tree Species Classifications in Central Europe. Remote Sensing 8, 166. https://doi.org/10.3390/rs8030166

Ismail, R., Mutanga, O., 2010. A comparison of regression tree ensembles: Predicting Sirex noctilio induced water stress in Pinus patula forests of KwaZulu-Natal, South Africa. International Journal of Applied Earth Observation and Geoinformation, Supplement Issue on "Remote Sensing for Africa – A Special Collection from the African Association for Remote Sensing of the Environment (AARSE)" 12, Supplement 1, S45–S51. https://doi.org/10.1016/j.jag.2009.09.004

Jaetzold, R., 1983. Natural conditions and farm management information. B (Central Kenya) and C (East Kenya). Farm management handbook of Kenya.

Jia, X., Richards, J.A., 1994. Efficient maximum likelihood classification for imaging spectrometer data sets. IEEE Transactions on Geoscience and Remote Sensing 32, 274–281.

Jung, H.G., Casler, M.D., 2006. Maize stem tissues: impact of development on cell wall degradability. Crop science 46, 1801.

Jusoff, K., Pathan, M., 2009. Mapping of individual oil palm trees using airborne hyperspectral sensing: an overview. Applied Physics Research 1, 15.

Kaufman, Y. J., Tanré, D., 1992. Atmospherically Resistant Vegetation Index (ARVI) for EOS-MODIS. IEEE Transactions on Geoscience and Remote Sensing 30 (2), 261–270.

Kavitha, K., Arivazhagan, S., 2010. A novel feature derivation technique for SVM based hyper spectral image classification. International Journal of Computer Applications 1, 25–31.

KNBS, 2010. 2009 Kenya Population and Housing Census Analytical Reports. Kenya National Bureau of Statistics.

Kumar, L., Schmidt, K., Dury, S., Skidmore, A., 2002. Imaging Spectrometry and Vegetation Science, in: Meer, F.D. van der, Jong, S.M.D. (Eds.), Imaging Spectrometry, Remote Sensing and Digital Image Processing. Springer Netherlands, pp. 111–155. https://doi.org/10.1007/978-0-306-47578-8_5

Landgrebe, D., 1999. Information extraction principles and methods for multispectral and hyperspectral image data. Information processing for remote sensing 82, 3–38.

Landgrebe, D.A., 2005. Signal theory methods in multispectral remote sensing. John Wiley & Sons.

Langley, S.K., Cheshire, H.M., Humes, K.S., 2001. A comparison of single date and multitemporal satellite image classifications in a semi-arid grassland. Journal of Arid Environments 49, 401–411.

Latif, Z.A., Zamri, I., Omar, H., 2012. Determination of tree species using Worldview-2 data, in: Signal Processing and Its Applications (CSPA), 2012 IEEE 8th International Colloquium On. IEEE, pp. 383–387.

Lenney, M.P., Woodcock, C.E., Collins, J.B., Hamdi, H., 1996. The status of agricultural lands in Egypt: the use of multitemporal NDVI features derived from Landsat TM. Remote Sensing of Environment 56, 8–20.

Li, L., Ustin, S.L., Lay, M., 2005. Application of multiple endmember spectral mixture analysis (MESMA) to AVIRIS imagery for coastal salt marsh mapping: a case study in China Camp, CA, USA. International Journal of Remote Sensing 26, 5193–5207.

Liaw, A., Wiener, M., 2002. Classification and regression by randomForest. R news 2, 18–22.

Lobell, D., Asner, G., 2003. "Hyperion Studies of Crop Stress in Mexico, in: Proceedings of the 12th Annual JPL Airborne Earth Science Workshop, Pasadena, CA.

Makori, D.M., Fombong, A.T., Abdel-Rahman, E.M., Nkoba, K., Ongus, J., Irungu, J., Mosomtai, G., Makau, S., Mutanga, O., Odindi, J., Raina, S., Landmann, T., 2017. Predicting Spatial Distribution of Key Honeybee Pests in Kenya Using Remotely Sensed and Bioclimatic Variables: Key Honeybee Pests Distribution Models. ISPRS International Journal of Geo-Information 6, 66. https://doi.org/10.3390/ijgi6030066

Mantero, P., Moser, G., Serpico, S.B., 2005. Partially supervised classification of remote sensing images through SVM-based probability density estimation. IEEE Transactions on Geoscience and Remote Sensing 43, 559–570.

Matsushita, B., Yang, W., Chen, J., Onda, Y., Qiu, G., 2007. Sensitivity of the Enhanced Vegetation Index (EVI) and Normalized Difference Vegetation Index (NDVI) to topographic effects: a case study in high-density cypress forest. Sensors 7(11), 2636–2651.

McCloy, K.R., Bøcher, P.K., 2007. Optimizing image resolution to maximize the accuracy of hard classification. Photogrammetric Engineering & Remote Sensing 73, 893–903.

Mercier, G., Girard-Ardhuin, F., 2006. Partially supervised oil-slick detection by SAR imagery using kernel expansion. IEEE Transactions on Geoscience and Remote Sensing 44, 2839–2846.

Mitchell, J.J., Glenn, N.F., Sankey, T.T., Derryberry, D.R., Germino, M.J., 2012. Remote sensing of sagebrush canopy nitrogen. Remote sensing of environment 124, 217–223.

Mumby, P.J., Edwards, A.J., 2002. Mapping marine environments with IKONOS imagery: enhanced spatial resolution can deliver greater thematic accuracy. Remote sensing of Environment 82, 248–257.

Mundt, C.W., Montgomery, K.N., Udoh, U.E., Barker, V.N., Thonier, G.C., Tellier, A.M., Ricks, R.D., Darling, R.B., Cagle, Y.D., Cabrol, N.A., 2005. A multiparameter wearable physiologic monitoring system for space and terrestrial applications. IEEE Transactions on Information Technology in Biomedicine 9, 382–391.

Mutanga, O., Adam, E., Cho, M.A., 2012. High density biomass estimation for wetland vegetation using WorldView-2 imagery and random forest regression algorithm. International Journal of Applied Earth Observation and Geoinformation 18, 399–406.

Nguyen, M.Q., Atkinson, P.M., Lewis, H.G., 2006. Superresolution mapping using a Hopfield neural network with fused images. IEEE Transactions on Geoscience and Remote Sensing 44, 736–749.

Nordberg, M.-L., Evertson, J., 2003. Monitoring change in mountainous dry-heath vegetation at a regional ScaleUsing multitemporal landsat TM data. AMBIO: A Journal of the Human Environment 32, 502–509.

Numata, I., Thenkabail, P.S., Lyon, J.G., Huete, A., 2012. Characterization on pastures using field and imaging spectrometers. Hyperspectral remote sensing of vegetation 207–226.

Okeke, F., Karnieli, A., 2006. Methods for fuzzy classification and accuracy assessment of historical aerial photographs for vegetation change analyses. Part I: Algorithm development. International journal of remote sensing 27, 153–176.

Omar, H., 2010. Commercial timber tree species identification using multispectral Worldview2 data. Digital Globe 8 Bands Research Challenge, 2–13.

Omoro, L., Starr, M., Pellikka, P.K., 2013. Tree biomass and soil carbon stocks in indigenous forests in comparison to plantations of exotic species in the Taita Hills of Kenya. Silva Fennica.

Omoro, L.M., Pellikka, P.K., Rogers, P.C., 2010. Tree species diversity, richness, and similarity between exotic and indigenous forests in the cloud forests of Eastern Arc Mountains, Taita Hills, Kenya. Journal of Forestry Research 21, 255–264.

Ouyang, Z.-T., Zhang, M.-Q., Xie, X., Shen, Q., Guo, H.-Q., Zhao, B., 2011. A comparison of pixel-based and object-oriented approaches to VHR imagery for mapping saltmarsh plants. Ecological Informatics 6, 136–146. https://doi.org/10.1016/j.ecoinf.2011.01.002

Padwick, C., Deskevich, M., Pacifici, F., Smallwood, S., 2010. WorldView-2 pan-sharpening, in: Proceedings of the ASPRS 2010 Annual Conference, San Diego, CA, USA.

Pang, H., Lin, A., Holford, M., Enerson, B.E., Lu, B., Lawton, M.P., Floyd, E., Zhao, H., 2006. Pathway analysis using random forests classification and regression. Bioinformatics 22, 2028–2036. https://doi.org/10.1093/bioinformatics/btl344

Peerbhay, K.Y., Mutanga, O., Ismail, R., 2013. Commercial tree species discrimination using airborne AISA Eagle hyperspectral imagery and partial least squares discriminant analysis (PLS-DA) in KwaZulu–Natal, South Africa. ISPRS Journal of Photogrammetry and Remote Sensing 79, 19–28.

Pellikka, P.A., Sarano, M.E., Nishimura, R.A., Malouf, J.F., Bailey, K.R., Scott, C.G., Barnes, M.E., Tajik, A.J., 2005. Outcome of 622 adults with asymptomatic, hemodynamically significant aortic stenosis during prolonged follow-up. Circulation 111, 3290–3295.

Pellikka, P.K., Lötjönen, M., Siljander, M., Lens, L., 2009. Airborne remote sensing of spatiotemporal change (1955–2004) in indigenous and exotic forest cover in the Taita Hills, Kenya. International Journal of Applied Earth Observation and Geoinformation 11, 221–232.

Peters, J., Baets, B.D., Verhoest, N.E.C., Samson, R., Degroeve, S., Becker, P.D., Huybrechts, W., 2007. Random forests as a tool for ecohydrological distribution modelling. Ecological Modelling 207, 304–318. https://doi.org/10.1016/j.ecolmodel.2007.05.011

Petropoulos, G.P., Manevski, K., Carlson, T.N., 2014. Hyperspectral remote sensing with emphasis on land cover mapping: From ground to satellite observations. John Wiley & Sons Inc.: Oxford, UK.

Piiroinen, R., Heiskanen, J., Mõttus, M., Pellikka, P., 2015. Classification of crops across heterogeneous agricultural landscape in Kenya using AisaEAGLE imaging spectroscopy data. International Journal of Applied Earth Observation and Geoinformation 39, 1–8. https://doi.org/10.1016/j.jag.2015.02.005

Pontius, R.G.J., Millones, M., 2011. Death to Kappa: birth of quantity disagreement and allocation disagreement for accuracy assessment. International Journal of Remote Sensing 32, 4407–4429. https://doi.org/10.1080/01431161.2011.552923

Prasad, R.P., Snyder, W.E., 2006. Diverse Trait-Mediated Interactions in a Multi-Predator, Multi-Prey Community. Ecology 87, 1131–1137. https://doi.org/10.1890/0012-9658(2006)87[1131:DTIIAM]2.0.CO;2

R. Core Team, 2014. R Development Core Team. R: A language and environment for statistical computing. R Foundation for Statistical Computing, Vienna, Austria; 2014.

Ritter, N., Logan, T., Bryant, N., 1988. Integration of neural network technologies with geographic information systems, in: Proceedings of the GIS Symposium: Integrating Technology and Geoscience Applications. pp. 102–103.

Roberts, D. A., Roth, K. L., Perroy, R. L., 2016. 14 Hyperspectral Vegetation Indices. Hyperspectral remote sensing of vegetation, pp 309.

Robledo, C., Fao, R. (Italy) F.R.D. eng, Forner, C., Cooperation, S.A. for D. and, Eng, B. (Switzerland), Cooperation, S.F. for D. and I., Eng, B. (Switzerland), 2005. Adaptation of forest ecosystems and the forest sector to climate change.

Rodríguez-Castañeda, G., Hof, A.R., Jansson, R., Harding, L.E., 2012. Predicting the Fate of Biodiversity Using Species' Distribution Models: Enhancing Model Comparability and Repeatability. PLOS ONE 7, e44402. https://doi.org/10.1371/journal.pone.0044402

Rogers, P.C., O'Connell, B., Mwang'ombe, J., Madoffe, S., Hertel, G., 2008. Forest health monitoring in the Ngangao forest, Taita Hills, Kenya: a five year assessment of change. Journal of East African Natural History 97, 3–17.

Salminen, H., 2004. A geographic overview of Taita Hills, Kenya, in: Taita Hills and Kenya, 2004. Seminar, Reports and Journal of a Field Excursion to Kenya. Expedition Reports of the Department of Geography, University of Helsinki. Citeseer, pp. 31–38.

Sarhrouni, El., Hammouch, A., Aboutajdine, D., 2012. Dimensionality reduction and classification feature using mutual information applied to hyperspectral images: a filter strategy based algorithm. arXiv preprint arXiv:1210.0052.

Schmidt, K.S., Skidmore, A.K., 2003. Spectral discrimination of vegetation types in a coastal wetland. Remote Sensing of Environment 85, 92–108. https://doi.org/10.1016/S0034-4257(02)00196-7

Shrestha, D.P., Zinck, J.A., 2001. Land use classification in mountainous areas: integration of image processing, digital elevation data and field knowledge (application to Nepal). International Journal of Applied Earth Observation and Geoinformation 3, 78–85.

Sohn, Y., Qi, J., 2005. Mapping detailed biotic communities in the Upper San Pedro Valley of southeastern Arizona using landsat 7 ETM+ data and supervised spectral angle classifier. Photogrammetric Engineering & Remote Sensing 71, 709–718.

Sohn, Y., Rebello, N.S., 2002. Supervised and unsupervised spectral angle classifiers. Photogrammetric engineering and remote sensing 68, 1271–1282.

Spruce, J.P., Sader, S., Ryan, R.E., Smoot, J., Kuper, P., Ross, K., Prados, D., Russell, J., Gasser, G., McKellip, R., Hargrove, W., 2011. Assessment of MODIS NDVI time series data products for detecting forest defoliation by gypsy moth outbreaks. Remote Sensing of Environment 115, 427–437. https://doi.org/10.1016/j.rse.2010.09.013

Stratoulias, D., Balzter, H., Sykioti, O., Zlinszky, A., Tóth, V.R., 2015. Evaluating Sentinel-2 for Lakeshore Habitat Mapping Based on Airborne Hyperspectral Data. Sensors 15, 22956–22969. https://doi.org/10.3390/s150922956

Strobl, C., Zeileis, A., 2008. Danger: High Power! – Exploring the Statistical Properties of a Test for Random Forest Variable Importance [WWW Document]. URL https://epub.ub.uni-muenchen.de/2111/ (accessed 1.7.17).

Subramanian, S., Gat, N., Sheffield, M., Barhen, J., Toomarian, N., 1997. Methodology for hyperspectral image classification using novel neural network, in: AeroSense'97. International Society for Optics and Photonics, pp. 128–137.

Tarabalka, Y., Benediktsson, J.A., Chanussot, J., 2009. Spectral–spatial classification of hyperspectral imagery based on partitional clustering techniques. IEEE Transactions on Geoscience and Remote Sensing 47, 2973–2987.

Thenkabail, P.S., Smith, R.B., De Pauw, E., 2000. Hyperspectral Vegetation Indices and Their Relationships with Agricultural Crop Characteristics. Remote Sensing of Environment 71, 158–182. https://doi.org/10.1016/S0034-4257(99)00067-X

Thulin, S., Hill, M.J., Held, A., Jones, S., Woodgate, P., 2012. Hyperspectral determination of feed quality constituents in temperate pastures: Effect of processing methods on predictive relationships from partial least squares regression. International Journal of Applied Earth Observation and Geoinformation 19, 322–334.

Toutin, T., 2004. Geometric processing of remote sensing images: models, algorithms and methods. International journal of remote sensing 25, 1893–1924.

Tso, B., Olsen, R.C., 2005. A contextual classification scheme based on MRF model with improved parameter estimation and multiscale fuzzy line process. Remote Sensing of Environment 97, 127–136.

UNDP, 2007. UNDP Annual Report 2007 [WWW Document]. UNDP. URL http://www.undp.org/content/undp/en/home/librarypage/corporate/undp_in_action_2007.html (accessed 3.13.18).

User Guides - Sentinel-2 MSI - Sentinel Online [WWW Document], n.d. URL https://sentinel.esa.int/web/sentinel/user-guides/sentinel-2-msi (accessed 5.1.17).

Vaiphasa, C., 2003. Innovative genetic algorithm for hyperspectral image classification, in: Proc. Int. Conf. Map Asia. p. 45.

van der Meer, F., 2006. The effectiveness of spectral similarity measures for the analysis of hyperspectral imagery. International journal of applied earth observation and geoinformation 8, 3–17.

Vapnik, V., 1998. Statistical learning theory. 1998. Wiley, New York.

Varshney, P.K., Arora, M.K., 2004. Advanced Image Processing Techniques for Remotely Sensed Hyperspectral Data. Springer Science & Business Media.

Vazquez, J., Perry, K., Kilpatrick, K., 1998. NOAA/NASA AVHRR Oceans Pathfinder sea surface temperature data set user's reference manual. Jet Propulsion Laboratory Tech. Rep. D-14070.

Veganzones, M.A., Simoes, M., Licciardi, G., Yokoya, N., Bioucas-Dias, J.M., Chanussot, J., 2016. Hyperspectral super-resolution of locally low rank images from complementary multisource data. IEEE Transactions on Image Processing 25, 274–288.

Voss, M., Sugumaran, R., 2008. Seasonal effect on tree species classification in an urban environment using hyperspectral data, LiDAR, and an object-oriented approach. Sensors 8, 3020–3036.

Wang, Q., Tenhunen, J.D., 2004. Vegetation mapping with multitemporal NDVI in North Eastern China transect (NECT). International Journal of Applied Earth Observation and Geoinformation 6, 17–31.

Wang, S., Wang, C., 2015. Research on dimension reduction method for hyperspectral remote sensing image based on global mixture coordination factor analysis. The International Archives of Photogrammetry, Remote Sensing and Spatial Information Sciences 40, 159.

Weber, R., 2006. Reach and grasp in the debate over the IS core: An empty hand? Journal of the Association for Information Systems 7, 28.

Wu, H., Li, Z.-L., 2009. Scale issues in remote sensing: A review on analysis, processing and modeling. Sensors 9, 1768–1793.

Wu, L.-X., Liang, B., Liu, X.-M., Zhang, Y., 2005. A spectral preservation fusion technique for remote sensing images. Journal of Surveying and Mapping 34(2), 118–122.

Xiao, L., Boyd, S., 2004. Fast linear iterations for distributed averaging. Systems & Control Letters 53, 65–78.

Xie, Y., Sha, Z., Yu, M., 2008. Remote sensing imagery in vegetation mapping: a review. J Plant Ecol 1, 9–23. https://doi.org/10.1093/jpe/rtm005

Xu, R., Wunsch, D., 2005. Survey of clustering algorithms. IEEE Transactions on neural networks 16, 645–678.

Yang, H., 1999. A back-propagation neural network for mineralogical mapping from AVIRIS data. International Journal of Remote Sensing 20, 97–110.

Yanqin, T., Ping, G., 2005. Comparative Studies on Dimension Reduction Methods for Multispectral Remote Sensing Image. Presented at the 3rd International Conference:

Sciences of Electronic, Technologies of Information and Telecommunications, March 27-31, 2005 – TUNISIA.

Yegnanarayana, B., 2009. Artificial neural networks. PHI Learning Pvt. Ltd.

Yin, J., Wang, Y., Hu, J., 2012. A new dimensionality reduction algorithm for hyperspectral image using evolutionary strategy. IEEE Transactions on Industrial Informatics 8, 935–943.

Zhang, J., Wu, J., Zhou, L., 2011. Deriving vegetation leaf water content from spectrophotometric data with orthogonal signal correction-partial least square regression. International journal of remote sensing 32, 7557–7574.

Zhang, Y., Atkinson, P.M., Ling, F., Wang, Q., Li, X., Shi, L., Du, Y., 2017. Spectral–Spatial Adaptive Area-to-Point Regression Kriging for MODIS Image Downscaling. IEEE Journal of Selected Topics in Applied Earth Observations and Remote Sensing 10, 1883–1896.

Zhou, H., Mao, Z., Wang, D., 2005. Classification of coastal areas by airborne hyperspectral image, in: Optical Technologies for Atmospheric, Ocean, and Environmental Studies. International Society for Optics and Photonics, pp. 471–476.

Zhu, L., Tateishi, R., 2006. Fusion of multisensor multitemporal satellite data for land cover mapping. International Journal of Remote Sensing 27, 903–918.